View metadata, citation and similar papers at core.ac.uk
brought to you by CORE
provided by UPCommons. Portal del coneixement obert de la UPC

MASTER'S DEGREE THESIS

Master of Science in Advanced Mathematics and Mathematical Engineering

Title: Non-Fourier Heat Conduction. The Maxwell-Cattaneo Equations

Author: Marc Calvo Schwarzwälder

Advisor: Tim Myers

Department: Matemàtica Aplicada I

Academic year: 2014-2015

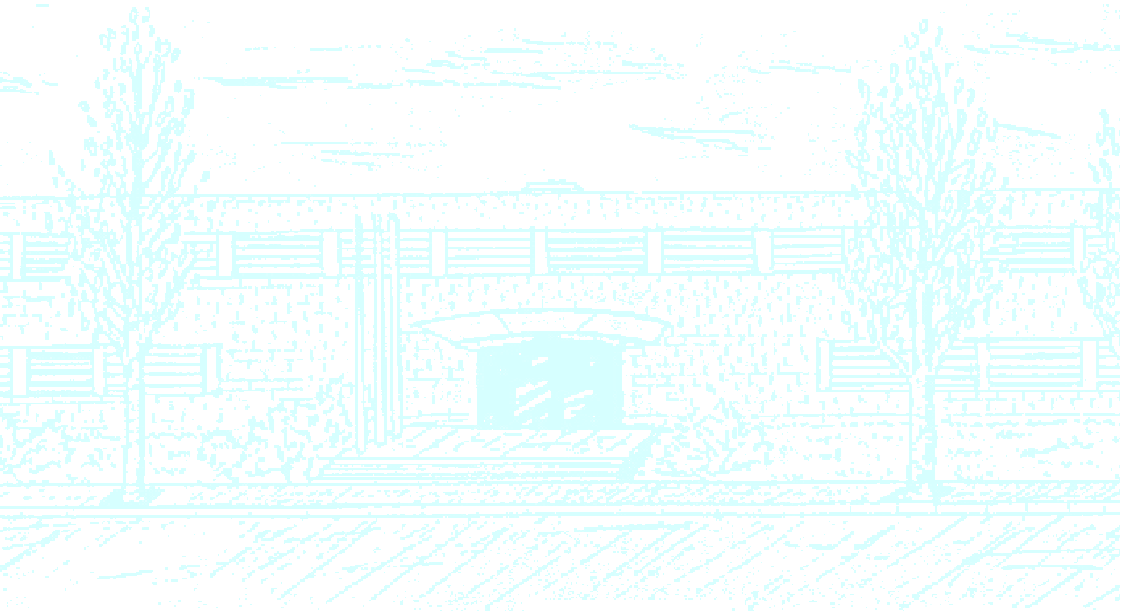

UNIVERSITAT POLITÈCNICA DE CATALUNYA
BARCELONATECH
Facultat de Matemàtiques i Estadística

Universitat Politècnica de Catalunya
Facultat de Matemàtiques i Estadística

Master's Degree Thesis

Non-Fourier Heat Conduction. The Maxwell-Cattaneo Equations

Marc Calvo Schwarzwälder

Advisor: Tim Myers

Departament de Matemàtica Aplicada I - UPC

To my family and friends.

Abstract

Key words: Thermal propagation, Parabolic heat equation, Non-Fourier heat conduction, Maxwell-Cattaneo equations, Hyperbolic heat equation

MSC 2010: 35K05, 35L15

The classical model proposed by Fourier over 200 years ago in order to describe the conduction of heat turns out to fail in some situations that are more and more frequent nowadays, for example those that involve short heating periods or extremely low temperatures. Cattaneo introduced the thermal relaxation time in order to provide a model that generalises the one by Fourier. This led to a hyperbolic equation for the temperature, introducing the idea of thermal waves and finite propagation time. In this dissertation we review some aspects on the classical and the hyperbolic models, with focus on the solution methods that have been used to deal with these problems.

Contents

1 Introduction **3**
- 1.1 Historical background and motivation 3
- 1.2 Conservation of energy 4

2 Fourier's theory on heat conduction **5**
- 2.1 Fourier's Law and the classical heat equation 5
- 2.2 Properties of the CHE 5
- 2.3 Solution methods 7
- 2.4 Results 11

3 The Maxwell-Cattaneo theory on heat conduction **15**
- 3.1 Cattaneo's law and the hyperbolic heat equation 15
- 3.2 Nondimensionalisation 16
- 3.3 Properties 17
- 3.4 Analytical expression for the heat flux 20
- 3.5 Frame-invariant formulation of the Maxwell-Cattaneo model 20
- 3.6 Solution Methods 22

4 Limit behaviour of HHE-solutions **33**
- 4.1 The Nagy-Ortiz-Reula Theorem 33
- 4.2 Modified Nagy-Ortiz-Reula Theorem 36
- 4.3 Conclusions 38

5 Laser heating of a thin film **41**
- 5.1 Model with Dirichlet boundary conditions 41
- 5.2 Model with Neumann boundary conditions 43
- 5.3 Model with an internal heat source 45
- 5.4 Model using the Maxwell-Cattaneo equations 48
- 5.5 Results 53

6 Heating of Biological Tissue **55**
- 6.1 Thermal models for biological tissue. Pennes bioheat equation 55
- 6.2 Mathematical study of RFH 56
- 6.3 Results 59

7 Conclusions **63**
7.1 Summary and results .. 63
7.2 Limitations and thermodynamical analysis .. 64
7.3 Further work .. 64

Bibliography **67**

Nomenclature and notation

c_p	specific heat at constant pressure (J/kgK)
k	thermal conductivity (W/Km)
k^{-1}	thermal resistivity (Km/W)
ρ	density (kg/m^3)
α	thermal diffusivity (m^2/s)
τ_0	thermal relaxation time (s)
c	speed of thermal wave (m/s)
ϵ	inverse of the speed of thermal wave (s/m)
$\partial_a f$, f_a, $f_{i,a}$	partial derivative with respect to a
T	temperature (K)
T_0, T_w, T_∞	reference temperatures (K)
$\mathbf{q}$, q	heat flux (W/m^2)
q_0	reference heat flux (W/m^2)
x	length variable (m)
L	reference length (m)
t	time variable (s)
t_0	reference time (s)
δ	heat penetration depth (m)
$\mathbf{a}$	vectorial quantity
a	scalar quantity

Special functions and transforms

δ_0	Dirac delta function
H	Heaviside function
J_0	Bessel function of 0^{th} order
$\mathcal{F}_y\{f\}$, $\hat{f}$	Fourier transform
$\mathcal{F}_x^{-1}\{f\}$, $\check{f}$	inverse Fourier transform
$\mathcal{L}_s\{f\}$, $\tilde{f}$	Laplace transform
$\mathcal{L}_s^{-1}\{f\}$	inverse Laplace transform

1
Introduction

1.1 Historical background and motivation

The classical theory of heat transport is based on Fourier's law, which states that the flow of heat is proportional to the temperature gradient. This assumption leads to the classical form of the heat equation, which has been successfully used to model the temperature in materials for over 200 years. However, as technology advances, situations arise where the standard heat equation is no longer accurate and certain accepted properties turn out to be invalid.

Experimental data and simulations have demonstrated that at the nanoscale, heat does not necessarily flow in the classical manner. For example, experiments of laser heating of ultrathin layers [19] or simulations of heat transport in solids using molecular dynamics [9] show dramatic discrepancies with respect to classical laws. This unpredictable behaviour makes the design stage of future nanoscale devices very difficult. Understanding heat transport at this scale and proposing modified versions of the classical equations (that prove to be valid) is a key point in order to ease the design of these future devices.

It turns out that that Fourier's law assumes an infinite speed of heat propagation, which means that any initial disturbance at any point is felt instantly in the whole medium. This behaviour is known as the 'Paradox of Heat Conduction', and contradicts the so called *principle of causality*, which states that information cannot travel faster than a finite speed.

Various attempts have been made to develop an accurate mathematical model for heat flow, and perhaps two of the most well-known are the Maxwell-Cattaneo and the Guyer-Krumhansl equations. The first introduces a relaxation time into the heat flow expression that has the effect of changing the governing equation to a form of wave equation, which then exhibits significantly different behaviour to the standard heat equation. The second introduces nonlocal effects that incorporate interesting new phenomena such as heat viscosity.

The aim of this dissertation is to give an overview of the Maxwell-Cattaneo equations, which after eliminating the heat flux yields a heat equation different to the classical heat equation. The structure of the dissertation is as follows:

- In chapter 2 we review the derivation of Fourier's equation and some of the methods used to compute the solution to problems that involve this equation.
- In chapter 3 we present the Maxwell-Cattaneo model, that arises from changing Fourier's law by introducing the thermal relaxation time as a parameter.
- In chapter 4 we study the relationship between the solutions of both models, and under which conditions we can assume that the solution to Fourier's model is the limit of the solution to the M-C equations when the relaxation time tends to 0.
- In chapters 5 and 6 we deal with two examples where the M-C model is considered.
- In the final chapter we give some conclusions and a discussion on the validity of the M-C model as a more accurate model to describe heat flow in certain situations.

1.2 Conservation of energy

Let us first introduce one of the main equations of this project, that will be important in deriving both of the models studied. This equation, known as the *conservation of energy*, states that the heat flux $\mathbf{q} = \mathbf{q}(\mathbf{x}, t)$ and temperature $T = T(\mathbf{x}, t)$ in a certain domain $\Omega \subseteq \mathbb{R}^n$ satisfy the relation

$$c_p \rho \frac{\partial T}{\partial t} + \nabla \cdot \mathbf{q} - S = 0, \tag{1.1}$$

where $S = S(\mathbf{x}, t)$ is an internal heat source. The quantities c_p and ρ are the specific heat and density of the medium respectively, and are assumed to be constant throughout the whole text. This equation is generally valid, i.e., it is not dependent on the model that is being used, and it will be the starting point for both models that we will study.

2

Fourier's theory on heat conduction

2.1 Fourier's Law and the classical heat equation

Fourier stated that heat propagation is governed in a domain Ω by the equation

$$\mathbf{q} = -k\nabla T, \tag{2.1}$$

where k is called the *thermal conductivity* and will be assumed to be constant in our study. This principle states that heat is always propagated from points with a higher temperature to points with a lower value.

Combining (1.1) and (2.1) we obtain the *classical heat equation (CHE)*

$$c_p\rho T_t - k\Delta T = S. \tag{2.2}$$

Consider now a given region $\Omega \subseteq \mathbb{R}^3$ with an initial temperature T_0, and whose boundary is heated to a fixed temperature T_w. The whole problem reads

$$\begin{cases} T_t - \alpha\Delta T = \dfrac{1}{c_p\rho}S & \text{in } \Omega,\ t > 0, \\ T(\mathbf{x}, 0) = T_0 & \text{in } \Omega, \\ T = T_w & \text{on } \partial\Omega,\ t > 0, \end{cases} \tag{2.3}$$

where the quantity $\alpha = k/c_p\rho$ is called the *thermal diffusivity*.

2.2 Properties of the CHE

Existence and uniqueness of solutions

One of the first properties that one has to check is the number of solutions that the problem has got. In case of the CHE, the solutions turn out to be unique after the following theorem.

Theorem 1 (Uniqueness of solutions to the CHE). *The problem given by*

$$\begin{cases} T_t - \alpha\Delta T = \dfrac{1}{c_p\rho}S & \textit{in } \Omega,\ t > 0, \\ T(\boldsymbol{x}, 0) = T_0 & \textit{in } \Omega, \\ T = T_w & \textit{on } \partial\Omega,\ t > 0, \end{cases} \tag{2.4}$$

has a unique solution.

Proof. Let u, v be two solutions to (2.5), and consider $w = u - v$, which trivially solves

$$\begin{cases} w_t - \Delta w = 0 & \text{in } \Omega,\ t > 0, \\ w(\mathbf{x}, 0) = 0 & \text{in } \Omega, \\ w = 0 & \text{on } \partial\Omega,\ t > 0. \end{cases} \tag{2.5}$$

Define now $E(t)$ as

$$E(t) = \frac{1}{2}\int_\Omega w^2 d\mathbf{x}, \tag{2.6}$$

whose derivative, denoted by $\dot{E}$, is given by

$$\begin{aligned} \dot{E} &= \textstyle\int_\Omega w\partial_t w d\mathbf{x} \\ &= \textstyle\int_\Omega w\Delta w d\mathbf{x} \\ &= \textstyle\int_{\partial\Omega} w\partial_n w d\mathbf{x} - \int_\Omega \|\nabla w\|^2 d\mathbf{x} \\ &= -\textstyle\int_\Omega \|\nabla w\|^2 d\mathbf{x} \\ &\leq 0, \end{aligned} \tag{2.7}$$

where we have used (2.5). Now, since $E(0) = \frac{1}{2}\int_\Omega w(\mathbf{x}, 0)^2 d\mathbf{x} = 0$, we deduce that $w = 0$ and consequently $u = v$.

□

Note that, in the case of Neumann or even mixed boundary conditions, the proof is analogous.

Existence of a Maximum Principle

Even if we cannot give the solution to a given problem, one can extract a lot of information concerning the solution itself just by analyzing the equation and the conditions that it has to satisfy. A very important property concerns the maximal and minimal values that the solution can take, and where it is allowed to take these values.

Theorem 2 (Maximum Principle)**.** *Let u be the solution to*

$$\begin{cases} u_t - \Delta u = 0 & \textit{in } \Omega,\ t > 0, \\ u(\boldsymbol{x}, 0) = g(\boldsymbol{x}) & \textit{in } \Omega. \end{cases} \tag{2.8}$$

Then u takes its maximal and minimal values either at $\partial\Omega$ or at $t = 0$.

Proof. See [1].

□

2.3 Solution methods

We have proved that the solution to the CHE is unique and that we can obtain its maximal and minimal values without computing it explicitely, but in practise one has to find the solution, or at least an approximation to it that is good enough. There are several methods to obtain either exact or approximate solutions, and it depends on each problem which solution method one should use. We will give a few examples, namely the Laplace transform and similarity variables to compute the exact solution, whilst we will use the separation of variables method and the heat balance integral method (HBIM) to obtain an approximate solution. A generalisation of the latter will be introduced in the next chapter, but it will also apply in this case when dealing with nonhomogeneous heat equations.

Exact Solution Methods

We will from now on consider the problem

$$\begin{cases} T_t - \alpha T_{xx} = 0, & x > 0,\ t > 0, \\ T(x,0) = T_0, & x > 0, \\ T(0,t) = T_w, & t > 0, \\ \lim\limits_{x\to\infty} T(x,t) = T_0, & t > 0, \end{cases} \tag{2.9}$$

where $T_w > T_0$. We define the following nondimensional variables

$$x' = \frac{x}{\gamma_x},\ t' = \frac{t}{\gamma_t},\ u' = \frac{T - T_0}{\gamma_T}, \tag{2.10}$$

where $\gamma_x = L$, $\gamma_t = L^2/\alpha$ and $\gamma_T = T_w - T_0$. The scaling parameter L is the typical length scale of the system. Applying these new variables, equations (2.9) reduce to

$$u_t - u_{xx} = 0, \tag{2.11}$$

$$u(x,0) = 0, \tag{2.12}$$

$$u(0,t) = 1, \tag{2.13}$$

$$\lim_{x\to\infty} u(x,t) = 0, \tag{2.14}$$

where we have dropped the primes to simplify notation.

Laplace transforms

Definition 1 (Laplace transforms on L^1)**.** If $f \in L^1(0,\infty)$ we define its *Laplace transform*

$$\mathcal{L}_t\{f\}(s) = \tilde{f}(s) := \int_0^\infty e^{-st} f(t)dt, \tag{2.15}$$

where s is a complex argument.

Using this transformation we can reduce (2.11)-(2.14) to a problem with an ordinary differential equation

$$\begin{aligned}&\tilde{u}_{xx} - s\tilde{u} = 0,\\ &\tilde{u}(0,s) = \tfrac{1}{s},\\ &\lim_{x\to\infty} \tilde{u}(x,s) = 0,\end{aligned} \tag{2.16}$$

whose general solution is given by

$$\tilde{u}(x,s) = Ae^{\sqrt{s}x} + Be^{-\sqrt{s}x}. \tag{2.17}$$

The transformed boundary conditions then imply $A = 0,\ B = 1/s$, and hence the solution to (2.16) is

$$\tilde{u}(x,s) = \frac{1}{s}e^{-\sqrt{s}x}. \tag{2.18}$$

In general, computing the inverse Laplace transform is tedious and not trivial, and even using numerical methods requires a lot of effort to compute the original function. In this case, the inverse transform is given by

$$u(x,t) = \operatorname{erfc}\left(\frac{x}{2\sqrt{t}}\right), \tag{2.19}$$

where erfc is the complementary error function

$$\operatorname{erfc}(x) = \int_x^\infty e^{-t^2}\,dt. \tag{2.20}$$

The next solution method will justify that $\{L\}_s^{-1}\tilde{u} = u$.

Similarity Solutions

Let us compute (2.19) again, but now using the method of similarity variables. Assume $u(x,t) = f(\eta)$ where $\eta = axt^b$. Quick computations yield

$$\begin{aligned}&u_t = abxt^{b-1}f_\eta,\\ &u_x = axt^b f_\eta,\\ &u_{xx} = a^2t^{2b}f_{\eta\eta},\end{aligned} \tag{2.21}$$

and hence (2.11)-(2.14) becomes

$$b\eta f_\eta = a^2t^{2b+1}f_{\eta\eta}. \tag{2.22}$$

Now we can remove the dependence on time by choosing $b = -1/2$, and setting $a = \sqrt{1/2}$, simplifies (2.22) to

$$f_{\eta\eta} + \eta f_\eta = 0. \tag{2.23}$$

After integrating twice we obtain

$$f(\eta) = C_1\operatorname{erf}(\eta) + C_2. \tag{2.24}$$

Using $u(x,t) = f\left(\frac{x}{2\sqrt{t}}\right)$, the boundary conditions (2.13) and (2.14) become

$$f(0) = 1,\ \lim_{\eta\to\infty} f(\eta) = 0, \tag{2.25}$$

and hence $C_1 = -1$ and $C_2 = 1$. Therefore

$$u(x,t) = f\left(\frac{x}{2\sqrt{t}}\right) = 1 - \operatorname{erf}(\eta), \tag{2.26}$$

which is equivalent to (2.19). Since the Laplace transform is an isomorphism [1], it turns out that

$$\mathcal{L}_s^{-1}\left\{\frac{1}{s}e^{-\sqrt{s}x}\right\} = \operatorname{erfc}\left(\frac{x}{2\sqrt{t}}\right). \tag{2.27}$$

Approximate Solution Methods

Heat Balance Integral Method

Let $\delta(t)$ be the point at which the changes in temperature from the initial value are negligible, i.e., the point such that $u(x,t) - u(x,0) \approx 0$ for all $x \geq \delta(t)$. Furthermore, let us substitute (2.14) with

$$u(\delta,t) = 0, \tag{2.28}$$

$$u_x(\delta,t) = 0, \tag{2.29}$$

where the second condition assures that the solution for $x < \delta$ joins smoothly the trivial solution for $x > \delta$. In the simplest form of HBIM, the solution is approximated by

$$u(x,t) = a_0(t) + a_1(t)\left(1 - \frac{x}{\delta}\right) + a_2(t)\left(1 - \frac{x}{\delta}\right)^2. \tag{2.30}$$

The degree of the polynomial is the lowest that one can choose, since a constant or linear polynomial does not satisfy all the boundary conditions of the problem. Using condition (2.28) yields $a_0 \equiv 0$, while $a_1 \equiv 0$ follows from condition (2.29). Finally, condition $u(0,t) = 1$ implies $a_2 \equiv 1$ and hence the approximation is given by

$$u(x,t) = \left(1 - \frac{x}{\delta}\right)^2, \tag{2.31}$$

where $\delta(t)$ is still to be determined. Now, let us compute δ by integrating equation (2.11) along the interval $[0,\delta]$,

$$\int_0^\delta u_t(x,t)dx = \int_0^\delta u_{xx}(x,t)dx. \tag{2.32}$$

Applying Leibniz's formula to (2.32) leads to

$$\frac{d}{dt}\int_0^\delta u(x,t)dx = \int_0^\delta u_t(x,t)dx + \delta' u(\delta,t), \tag{2.33}$$

and, using (2.28) we obtain

$$\int_0^\delta u_t(x,t)dx = \frac{d}{dt}\int_0^\delta u(x,t)dx. \tag{2.34}$$

The right hand side of (2.32) can be simplified using the Fundamental Theorem of Calculus:

$$\begin{aligned}\textstyle\int_0^\delta u_{xx}(x,t)dx &= u_x(\delta,t) - u_x(0,t)\\ &= -u_x(0,t),\end{aligned} \tag{2.35}$$

where we have used (2.29). Therefore, equation (2.32) simplifies to

$$\frac{d}{dt}\int_0^{\delta} u(x,t)dx = -u_x(0,t), \tag{2.36}$$

and using (2.31) we obtain

$$\delta' = \frac{6}{\delta}. \tag{2.37}$$

Applying the initial condition $\delta(0) = 0$ we finally find the expression

$$\delta(t) = \sqrt{12t}, \tag{2.38}$$

and thus the HBIM solution to (2.11)-(2.14) is given by

$$u(x,t) = \left(1 - \frac{x}{\sqrt{12t}}\right)^2. \tag{2.39}$$

Separation Of Variables

This solution method actually yields an exact solution of the CHE, but it is considered as an approximate method because the solution is given in terms of an series that in practise has to be truncated at some point. Consider problem (2.11)-(2.14) in a finite domain, i.e., let $0 \leq x \leq L$, and therefore substitute condition (2.14) with

$$u(1,t) = 0,\ t > 0. \tag{2.40}$$

where we have already used the nondimensional variables (2.10). To make the boundary conditions homogeneous, let $w = u + (x - 1)$. The equation for w is

$$w_t - w_{xx} = 0, x > 0,\ t > 0, \tag{2.41}$$

$$w(x,0) = x - 1, x > 0, \tag{2.42}$$

$$w(0,t) = 0, t > 0, \tag{2.43}$$

$$w(1,t) = 0, t > 0, \tag{2.44}$$

Now let $w(x,t) = X(x)T(t)$, which turns (2.41) into

$$\frac{X''}{X} = \frac{T'}{T}. \tag{2.45}$$

Since both sides of this equation are independent of each other, both sides must be constant, say $\lambda \in \mathbb{R}$. It turns out that $\lambda \geq 0$ yields only trivial solutions $w \equiv 0$, and hence we let $\lambda = -\mu^2$. We therefore obtain two independent equations

$$T' + \mu^2 T = 0, \tag{2.46}$$

$$X'' + \mu^2 X = 0. \tag{2.47}$$

The general solution to (2.46) is given by

$$T(t) = Ae^{-\mu^2 t}, \tag{2.48}$$

whilst for (2.47) we obtain

$$X(x) = C_1 \cos(\mu x) + C_2 \sin(\mu x). \tag{2.49}$$

Using conditions (2.43) and (2.44) we find that $X(0) = X(1) = 0$ and therefore $C_1 = 0$. Since we do not want trivial solutions, the second condition implies $\sin(\mu) = 0$, and hence $\mu = \mu_n = n\pi$ for $n = 1, 2, 3....$ Since (2.41) is linear, adding the solutions, we obtain again another solution. This property is called the ***superposition principle***. Therefore, we have that the general solution to (2.9) is given by

$$w(x,t) = \sum_{n=1}^{\infty} A_n e^{-(n\pi)^2 t} \sin(n\pi x). \tag{2.50}$$

Using (2.42) it turns out that the coefficients A_n have to be the Fourier coefficients of the initial condition $w(x, 0) = x - 1$, i.e.,

$$A_n = 2\int_0^1 (x-1)\sin(n\pi x)dx = -\frac{2}{n\pi}. \tag{2.51}$$

The final solution to the problem is

$$u(x,t) = \sum_{n=1}^{\infty} A_n e^{-(n\pi)^2 t} \sin(n\pi x) + 1 - x. \tag{2.52}$$

2.4 Results

The accuracy of the approximate methods has been analyzed through figures 2.1 and 2.2. The error is computed via the formula

$$E = |u_{exact} - u_{approx}|, \tag{2.53}$$

where the approximate solution is once given by separation of variables (dashed line in figures 2.1 and 2.2) and by the HBIM (dotted line in figures 2.1 and 2.2). In the separation of variables solution, the spatial variable has been taken in the interval $[0, 10]$, thus $L = 10m$. For higher values the solution is assumed to be zero.

In figure 2.1 we notice that, for small values of t, the HBIM solution shows excellent agreement with the exact solution. On the other hand, the separable solution oscilates and displays a huge error in comparison to the HBIM solution. The reason for this behaviour is that we are approximating the separable solution through a finite sum of continuous functions, since we are not able to compute the whole series. For instance, in these plots we have approximated the solution with the first 50 terms of the series in (2.52). Therefore we are plotting a continuous function that is asumed to approach a discontinuity at $(x, t) = (0, 0)$ due to the initial conditions, that impose $u(x, 0) = 0$ and $u(0, t) = 1$ at the same time. This is known as the *Gibbs phenomenon*. Observe from the plot for higher values of t in figure 2.1, that this phenomenon is only noticed for early times.

By contrast, notice that in the case of the intermediate time solution ($t = 3s$), both methods seem to approach the exact solution quite well, although the separable solution seems to give a better approximation. However, the maximum error of the HBIM solution is just marginally more than 3%.

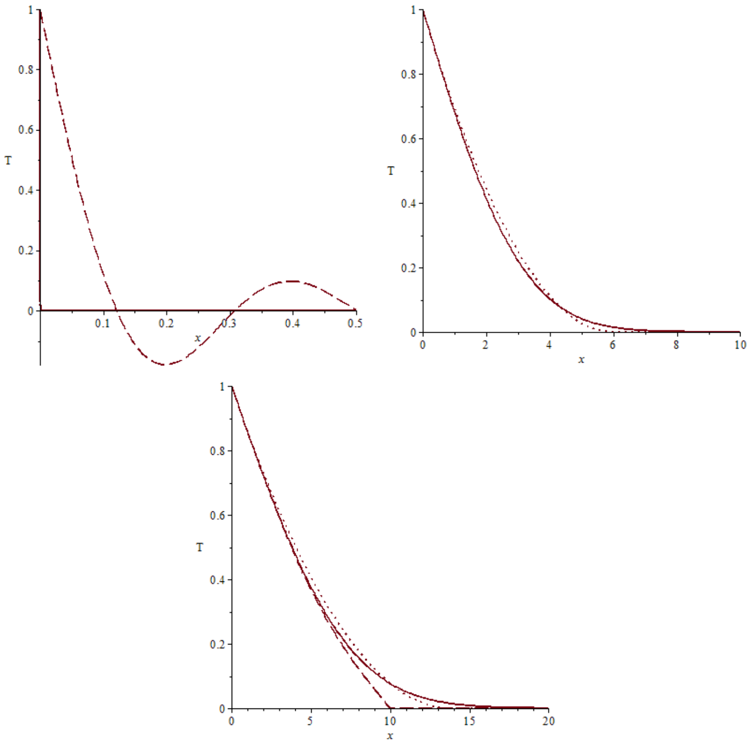

Figure 2.1: Temperature profiles for $t = 10^{-7}s$, $t = 3s$ and $t = 16s$ respectively. The solid line displays the exact solution, whilst the dashed line corresponds to the solution computed by separation of variables and the dotted line to the HBIM solution.

For $t = 16s$ we see that the separable solution is again a bad approximation of the exact solution, whilst the HBIM solution still shows an maximum error of 3%. The reason for this can be deduced from figure 2.1. Since the separable solution is asumed to be zero for $x > L$ and $L = 10$ in this case, we have to rescale the spatial variable again to obtain a more accurate solution. For instance, if we now set $L = 20m$, the comparison in figure 2.3 shows that after the rescaling of the spatial variable, the separable solution becomes again a good approximation of the exact solution.

The conclusion that one may draw from these results is that separation of variables yields a good approach to the exact solution, as long as the spatial variable is well scaled. When dealing with early times the Gibbs phenomenon arises and the separable solution is no longer accurate. On the other hand, the HBIM seems to be a good approach to the exact solution for all times and one does not have to deal with rescalings of the spatial variables. One of the main differences between both methods is that the finite space is predetermined in the first one, whilst the HBIM calculates a new interval in every time step. However, if the space is properly scaled the separable solution is more accurate than the HBIM solution. Nevertheless, the efficiency of the HBIM can be improved in several ways [8].

Notice from the expression of the exact solution in (2.19) that $u(x, 0) = 0$ for $x > 0$ but $u(x, t) > 0$ for $x, t > 0$, i.e., observe that the initial disturbance in the origin is felt instantly in the whole medium. We will try to overcome this problem in the next

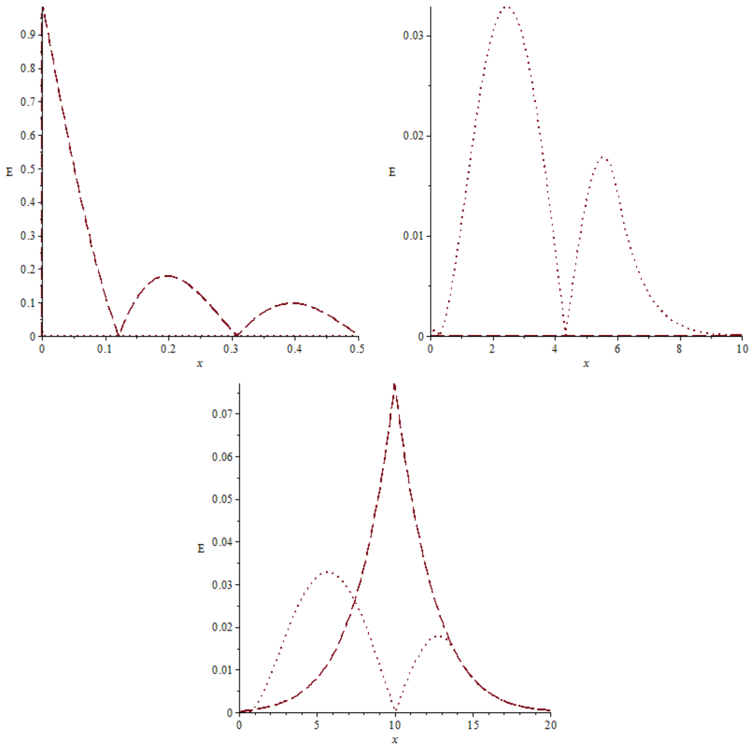

Figure 2.2: Absolute error for $t = 10^{-7}s$, $t = 3s$ and $t = 16s$ respectively, where the dashed line corresponds to the separation of variables and the dotted line refers to the HBIM solution.

chapter.

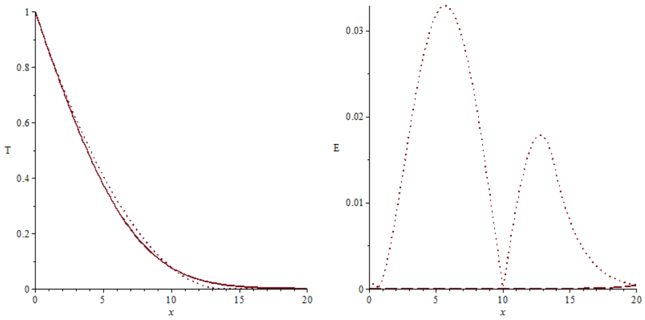

Figure 2.3: Temperature profile and error at $t = 16$ after rescaling the spatial variable in the separable variable.

3

The Maxwell-Cattaneo theory on heat conduction

3.1 Cattaneo's law and the hyperbolic heat equation

The Italian mathematician Carlo Cattaneo [5] tried to overcome the problem of infinite speed of heat propagation by deriving a new equation to relate the heat flux q and the temperature T, and hence replace Fourier's law. Cattaneo introduced the *thermal relaxation characteristic time* τ_0, which is interpreted by Chandrasekharaiah as *"the time lag required to establish steady heat conduction in a volume element once a temperature gradient has been imposed across it"* [13], i.e., the time needed to reach thermodynamic stability. Therefore, the relaxation time introduces the idea of finite speed of heat propagation. The equation proposed by Cattaneo is

$$\mathbf{q} + \tau_0 \mathbf{q}_t = -k \nabla T, \tag{3.1}$$

where the new term is called *thermal inertia* [11]. The value of τ_0 obviously depends on the material being considered. It has been given experimentally for a large number of materials, turning out to be very small, of the order of picoseconds, in the case of most metals, but up to $100s$ for some biological tissues [11].

Equations (1.1) and (3.1) form the *Maxwell-Cattaneo equations.* The British physicist Maxwell got his name attached to the equation because he had derived a similar equation when providing a mathematical basis for the kinetic theory of gases [7]. In many references, these equations are also known as the *Maxwell-Cattaneo-Vernotte equations* in honor of the French mathematician Pierre Vernotte, who derived the same equations almost at the same time [6].

We now derive a unique equation for T in one-dimensional space, when q is defined by (3.1). Consider (1.1) at time $t + \tau_0$, i.e.,

$$c_p \rho T_t(x, t + \tau_0) + q_x(x, t + \tau_0) - S(x, t + \tau_0) = 0, \tag{3.2}$$

and apply a Taylor series expansion to order τ_0 to obtain

$$c_p\rho\partial_t\left(T(x,t)+\tau_0 T_t(x,t)\right)+\partial_x\left(q(x,t)+\tau_0 q_t(x,t)\right)-\left(S(x,t)+\tau_0 S_t(x,t)\right)=0, \quad (3.3)$$

which, using (3.1), leads to

$$\tau_0 T_{tt}+T_t-\alpha T_{xx}=\frac{1}{c_p\rho}\left(S+\tau_0 S_t\right). \quad (3.4)$$

In this context, equation (3.4) is called the *hyperbolic heat equation (HHE)*, due to the second derivatives involved it has the same hyperbolic character as the classical wave equation

$$T_{tt}-c^2T_{xx}=0. \quad (3.5)$$

In fact, assuming $S\equiv 0$ and if one lets $c^2=\alpha/\tau_0$, then (3.4) can be transformed into

$$T_{tt}+\frac{1}{\tau_0}T_t-c^2T_{xx}=0, \quad (3.6)$$

which describes the damped propagation of a wave. This scenario encourages the idea of *thermal wave* that propagates heat with a finite speed. In fact, if we compute the dimensions of c

$$[c^2]=\frac{[\alpha]}{[\tau_0]}=\frac{m^2s^{-1}}{s}=\left(\frac{m}{s}\right)^2. \quad (3.7)$$

we observe that c has the same dimensions as a velocity. In fact, c is called the *speed of second sound* [3], and it represents the speed of propagation of a thermal wave in the medium. The definition of second sound is due to the fact that it is generally not equal to the speed of sound in the medium. Moreover, it has been experimentally found that in liquid Helium II, for instance, the speed of heat is at least one order of magnitude less than the speed of sound [14].

Notice that as $\tau_0\to 0$ we recover the infinite speed of propagation and the equation turns out to be (2.2) again, hence we recover Fourier's model. Cattaneo's model is therefore consistent in this sense.

It is remarkable the fact that in this model we have to introduce an *initial thermal velocity* $T_t(x,t)$. This idea was completely absent in Fourier's model, but becomes important in this case. One could wonder if, for instance, the solution to (3.4) coincides in the limit as $\tau_0\to 0$ with the solution to (2.2), or if this might depend on the initial velocity that one has assumed for the hyperbolic model.

3.2 Nondimensionalisation

As in the case of the previous model, let us first reduce the number of parameters in our problem. Consider, for instance, the initial value problem

$$\begin{cases} \tau_0 T_{tt}+T_t-\alpha T_{xx}=0 & 0<x<L,\ t>0,\\ T(x,0)=T_0 & 0<x<L,\\ T_t(x,0)=0 & 0<x<L, \end{cases} \quad (3.8)$$

where some boundary conditions still have to be imposed. The initial thermal velocity has been chosen to be 0 because the system is initially assumed to be in equilibrium.

Let us apply the dimensionless variables (2.10) with $\gamma_x = L$ and $\gamma_t = L^2/\alpha$, whilst γ_T is a characteristic temperature related to the boundary conditions. Upon neglecting the prime notation the dimensionless equation for u is

$$\epsilon_0 u_{tt} + u_t - u_{xx} = 0, \tag{3.9}$$

with $\epsilon_0 = \alpha\tau_0/L^2$. Notice that typically $\alpha \sim 10^{-7}$, hence if we assume, for instance, $\tau_0 \sim 10^{-5}$ then $\epsilon \ll 1$ unless $L \sim 10^{-6}$. Therefore the term u_{tt} can be neglected in many cases, as long as the considered length scale is large enough. On the other hand, materials such as sand or $NaCO_3$ show larger values for τ_0 [13], and hence the wave-term cannot be eliminated in those cases.

During further studies we will give other choices of nondimensional variables. For instance, introducing the relaxation time into our nondimensional variables yields an equation without any parameter.

3.3 Properties

Solution Structure Theorem

It turns out that the solutions to the HHE can be expressed in terms of three solutions to easier problems, and which can reduce considerably the difficulty of the problem. Consider the general one-dimensional problem

$$\begin{cases} \epsilon_0 u_{tt} + u_t - u_{xx} = S, & 0 < x < 1,\ t > 0, \\ au(0,t) + bu_x(0,t) = cu(1,t) + du_x(1,t) = 0, & t > 0, \\ u(x,0) = f(x),\ u_t(x,0) = g(x), & 0 < x < 1, \end{cases} \tag{3.10}$$

where $a, b, c, d \in \mathbb{R}$ are the general coefficients of the boundary conditions. The following result gives a general description of the solution to (3.10).

Theorem 3. *Let $\phi \in L^2$ be arbitrary, we define $W_\phi(x,t)$ to be the solution to*

$$\begin{cases} \epsilon_0 u_{tt} + u_t - u_{xx} = 0, & 0 < x < 1,\ t > 0, \\ au(0,t) + bu_x(0,t) = cu(1,t) + du_x(1,t) = 0, & t > 0, \\ u(x,0) = 0,\ u_t(x,0) = \phi(x), & 0 < x < 1. \end{cases} \tag{3.11}$$

Then the solution to (3.10) is

$$u(x,t) = \left(\epsilon_0^{-1} + \partial_t\right) W_f + W_g + \int_0^t W_{\tilde{S}}(x,t;s)ds = u_1(x,t) + u_2(x,t) + u_3(x,t), \tag{3.12}$$

where $W_{\tilde{S}}(x,t;s)$ solves

$$\begin{cases} \epsilon_0 u_{tt} + u_t - u_{xx} = 0, & 0 < x < 1,\ t > s, \\ au(0,t) + bu_x(0,t) = cu(1,t) + du_x(1,t) = 0, & t > s, \\ u(x,s;s) = 0,\ u_t(x,s;s) = \tilde{S}(x,s), & 0 < x < 1, \end{cases} \tag{3.13}$$

where $\tilde{S} = S/\epsilon_0$.

Proof. Let us show that u_1 solves

$$\begin{cases} \epsilon_0 u_{tt} + u_t - u_{xx} = 0, & 0 < x < 1,\ t > 0, \\ au(0,t) + bu_x(0,t) = cu(1,t) + du_x(1,t) = 0, & t > 0, \\ u(x,0) = f,\ u_t(x,0) = 0, & 0 < x < 1. \end{cases} \tag{3.14}$$

The equation is satisfied since it can be rewritten as

$$(\epsilon_0^{-1} + \partial_t)\left(\epsilon_0 \partial_t^2 W_f(x,t) + \partial_t W_f(x,t) - \partial_x^2 W_f(x,t)\right) = 0. \tag{3.15}$$

On the other hand, due to the linear character of the boundary conditions, it is trivial to see that the boundary conditions are also satisfied. A few computations yield

$$\begin{aligned} u_1(x,0) &= \epsilon_0^{-1} W_f(x,0) + \partial_t W_f(x,0) = f(x), \\ u_{1,t}(x,t) &= \left(\epsilon_0^{-1}\partial_t + \partial_t^2\right) W_f(x,0) = \epsilon_0 \partial_x^2 W_f(x,0) = 0, \end{aligned} \tag{3.16}$$

where we have used that $W_f(x,0) = 0$ and $\partial_t W_f(x,0) = f(x)$.

The derivatives of u_3 are

$$\begin{aligned} u_{3,t} &= \int_0^t \partial_t W_{\tilde{S}}(x,t;s)ds, \\ u_{3,tt} &= \tfrac{1}{\epsilon_0} S(x,t) + \int_0^t \partial_t^2 W_{\tilde{S}}(x,t;s)ds, \\ u_{3,xx} &= \int_0^t \partial_x^2 W_{\tilde{S}}(x,t;s)ds \end{aligned} \tag{3.17}$$

where we have used $W_{\tilde{S}}(x,t;t) = 0,\ \partial_t W_{\tilde{S}}(x,t;t) = \tilde{S}(x,t)$. Therefore, u_3 is the solution to

$$\begin{aligned} \epsilon_0 u_{3,tt} + u_{3,t} - u_{3,xx}^3 &= S(x,t) + \int_0^t (\epsilon_0 \partial_t^2 + \partial_t - \partial_{xx}) W_{\tilde{S}}(x,t;s)ds \\ &= S(x,t). \end{aligned} \tag{3.18}$$

since $W_{\tilde{S}}$ satisfies

$$\epsilon_0 \partial_t^2 W_{\tilde{S}} + \partial_t W_{\tilde{S}} - \partial_x^2 W_{\tilde{S}} = 0. \tag{3.19}$$

The boundary conditions are trivially satisfied since the integral is a linear operator, and finally notice that $u_3(x,0) = u_{3,t}(x,0) = 0$ follows directly from the definition of u_3 and $u_{3,t}$. Now, since the HHE is linear, observe that $u = u_1 + u_2 + u_3$ is indeed the solution to (3.10).

□

Notice that theorem 3 does not assure that the solution exists. However, it reduces the initial problem (3.10) to three problems that are, in principle, easier to solve, since the initial temperature and the heat source are trivial in these cases.

Remarks regarding the Maximum Principle

Since (3.4) is principally a damped wave equation, there is automatically an important difference with the classical heat equation, the fact that the speed of heat propagation is not infinite anymore. On the other hand, since we now have to consider an initial velocity $u_t(x,0)$, intuitively we notice that the properties of the classical equation, such as the maximum principle, will not hold anymore, since a positive initial velocity would increase the temperature in the medium for $t > 0$. Consider, for instance, the nondimensional problem

$$\begin{cases} \epsilon_0 u_{tt} + u_t - u_{xx} = 0, & 0 < x < 1,\ t > 0, \\ u(x,0) = sin(\pi x), & 0 < x < 1, \\ u_t(x,0) = x(1-x), & 0 < x < 1, \\ u(0,t) = u(1,t) = 0, & t > 0, \end{cases} \tag{3.20}$$

Notice that the initial thermal velocity is maximal in the center of the interval $[0,1]$. Figure 3.1 shows that the temperature in the centre is higher at $t = 0.01$ than initially. It is therefore clear that in this situation the maximum principle cannot hold.

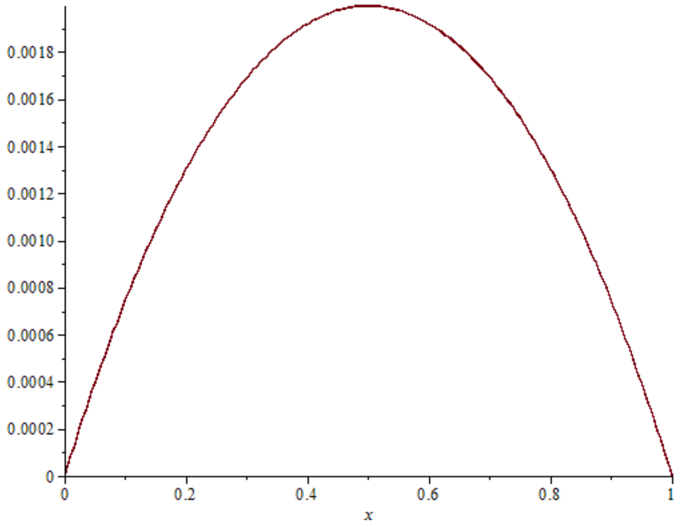

Figure 3.1: Plot of the difference $u(x,0.01) - u(x,0)$, where u is the solution to (3.20) when $\epsilon_0 = 1$.

Existence and uniqueness of solutions to the HHE

Although existence is not guaranteed, the following result shows that solutions are unique, provided they exist.

Theorem 4 (Uniqueness of solutions to the hyperbolic heat equation)**.** *The problem*

$$\begin{cases} \epsilon_0 u_{tt} + u_t - u_{xx} = f & 0 < x < 1,\ t > 0, \\ u(x,0) = g_1(x) & 0 < x < 1, \\ u_t(x,0) = g_2(x) & 0 < x < 1, \\ u(0,t) = h_1(t) & t > 0, \\ u(1,t) = h_2(t) & t > 0. \end{cases} \tag{3.21}$$

has, at most, one smooth solution.

Proof. Analogous to the proof of theorem 1.

□

3.4 Analytical expression for the heat flux

In this dissertation the heat flux $\mathbf{q}$ is also an unknown function that depends on the model chosen. For instance, we define $\mathbf{q_F}$ and $\mathbf{q_{MC}}$ as the heat fluxes corresponding to Fourier's and the Maxwell-Cattaneo's models, respectively.

Whilst the expression of $\mathbf{q_F}$ is given by (2.1), $\mathbf{q_{MC}}$ still has to be computed after solving the hyperbolic equation (3.4), since it obeys the Maxwell-Cattaneo law, i.e., it is the solution to (3.1). Assuming that the initial heat flux is zero, then $\mathbf{q_{MC}}$ is the solution to

$$\begin{cases} \mathbf{q_{MC}} + \tau_0 \partial_t \mathbf{q_{MC}} = -k\nabla T, \\ \mathbf{q_{MC}}(0) = 0. \end{cases} \tag{3.22}$$

From the theory of linear differential equations we know that the solution to the problem above is given by

$$\mathbf{q_{MC}}(\mathbf{x},t) = -\frac{k}{\tau_0}\int_0^t e^{-(t-s)/\tau_0}\nabla T(\mathbf{x},s)ds, \tag{3.23}$$

and therefore $\mathbf{q_{MC}}$ depends on the full history of the temperature gradient up to the present moment. Notice that this does not happen in the previous case, where the the heat flux given in (2.1) does not show such a property of having "memory".

3.5 Frame-invariant formulation of the Maxwell-Cattaneo model

We will now highlight a further model due to Christov [11], but without going too deep into it, since it does not apply with our considerations. Further information can be found in the references.

Consider a problem of heat transfer in a moving medium as, for instance, a rotating fluid. In this scheme, Christov *et al.* [10] proved that the Maxwell-Cattaneo model is not invariant under Galilean transformations, and hence the equations and their solution change as one considers different moving frames. Therefore, a more complete formulation is required.

Definition 2 (Material derivative)**.** Assume that the medium is moving with a certain velocity $\nu(\mathbf{x},t)$. Then, the *material* or *total derivative* of function $f(\mathbf{x},t)$ is

$$\frac{Df}{Dt} := f_t + \nu \cdot \nabla f. \tag{3.24}$$

The material derivative states that the rate of change of a certain quantity at a given point x_0 is due to two processes. On one hand, due to the change in that point, i.e., the partial derivative with respect to time. On the other hand, due to the fact that a different quantity is transported to x_0 from other points in its neighbourhood, which is described by the second term in (3.24).

The first change introduced by Christov is the replacement of the mere partial time derivative of (1.1) with the material derivative, i.e.,

$$c_p\rho T_t + \nu \cdot \nabla T + \nabla \cdot \mathbf{q} = 0. \tag{3.25}$$

Notice that, if $\nu \equiv 0$, we recover (1.1).

Definition 3 (Vector density)**.** We call a mechanical quantity $\mathbf{A}$, parametrized simultaneously by $\mathbf{x}$ and $\mathbf{x}'$, a *vector density*, iff $\mathbf{A}$ is invariant under coordinate transformations, i.e., if the following equation holds

$$\int_D \mathbf{A} d\mathbf{x} = \int_{D'} \mathbf{A} d\mathbf{x}'. \tag{3.26}$$

Notice that $\mathbf{q}$ is therefore a vector density, since it is physically obvoious that the heat flux across a given section is invariant with respect to the parametrization chosen.

Definition 4 (Upper convected time derivative)**.** Let $\mathbf{A}$ be a vector density, the quantity

$$\frac{\mathfrak{d}\mathbf{A}}{\mathfrak{d}t} := \mathbf{A}_t + \nu \cdot \nabla \mathbf{A} - \mathbf{A} \cdot \nabla \nu + (\nabla \cdot \nu) \cdot \mathbf{A}, \tag{3.27}$$

is called the *upper convected time derivative* for $\mathbf{A}(\mathbf{x}, t)$ [11].

If we replace $\mathbf{q}_t$ in (3.1) with $\frac{\mathfrak{d}\mathbf{q}}{\mathfrak{d}t}$ we obtain

$$\mathbf{q} + \tau_0 \left(\mathbf{q}_t + \nu \cdot \nabla \mathbf{q} - \mathbf{q} \cdot \nabla \nu + (\nabla \cdot \nu) \cdot \mathbf{q}\right) = -k\nabla T. \tag{3.28}$$

Equations (3.25) and (3.28) are known as the *Christov-Cattaneo equations.* Let us reduce the spatial variable to one for simplicity, then the C-C equations are

$$\begin{cases} c_p\rho\left(T_t + vT_x\right) = -q_x, \\ q + \tau_0\left(q_t + vq_x\right) = -kT_x. \end{cases} \tag{3.29}$$

Again, one can derive a single equation for the temperature. We differentiate the latter equation of (3.29) to obtain

$$q_x + \tau_0\left(q_{tx} + v_x q_x + v q_{xx}\right) = -kT_{xx}, \tag{3.30}$$

therefore, using the first equation of (3.29) we obtain

$$(1 + \tau_0 v_x)T_t + \left[v + \tau_0\left(v_t + 2vv_x\right)\right]T_x + 2\tau_0 vT_{tx} + \tau_0 T_{tt} + \tau_0 v^2 T_{xx} = \alpha T_{xx}. \tag{3.31}$$

To show that (3.31) is Galilean invariant, let us introduce the following change of variables, corresponding to a frame, moving with constant velocity V,

$$y = x - Vs, \; s = t, \; \Theta(y, s) = T(x, t), \; v = u + V. \tag{3.32}$$

It follows that

$$\begin{aligned} &T_t = \Theta_s - V\Theta_y, \\ &T_{tt} = \Theta_{ss} - 2V\Theta_{sy} + V^2\Theta_{yy}, \\ &T_{tx} = \Theta_{sy} - V\Theta_{yy}, \\ &T_x = \Theta_y, \\ &T_{xx} = \Theta_{yy} \\ &v_x = u_y, \\ &v_t = u_s - Vu_y. \end{aligned} \tag{3.33}$$

and hence, substituting the terms in (3.31) we obtain, after reordering and canceling terms,

$$(1+\tau_0 u_y)\Theta_s + \left[u + \tau_0 \left(u_s + 2uu_y\right)\right]\Theta_y + 2\tau_0 u\Theta_{sy} + \tau_0 u^2 \Theta_{yy} = \alpha\Theta_{yy}, \tag{3.34}$$

i.e., the same equation as (3.31) but in the new variables of the moving frame.

The C-C equations are widely used in heat transfer problems that involve a moving medium [12]. However, in our dissertation we will assume that the medium is not moving, i.e., $v \equiv 0$. In this case the C-C equations (3.31) reduce to the M-C equations (1.1) and (3.1).

3.6 Solution Methods

As in the previous chapter, let us now present some solution methods that are actually used to solve problems involving the Maxwell-Cattaneo equations and the resulting hyperbolic heat equation for the temperature. We will use a separation of variables method which is adapted for the HHE. Two generalisations of this method will then be introduced to solve nonhomogeneous problems, and finally we will highlight the Fourier transform method as a technique to obtain exact solutions.

Approximate Solution Methods

Separation of variables

Let us consider the nondimensional Cauchy problem given by

$$\begin{cases} \epsilon_0 u_{tt} + u_t - u_{xx} = 0 & 0 < x < 1,\ t > 0, \\ u(x,0) = f(x) & 0 < x < 1, \\ u_t(x,0) = g(x) & 0 < x < 1, \\ u(0,t) = u(1,t) = 0 & t > 0, \end{cases} \tag{3.35}$$

and assume that u is of the form

$$u(x,t) = \sum_{n=1}^{\infty} X(x)T(t). \tag{3.36}$$

This leads to

$$\epsilon_0 XT'' + XT' - X''T = 0, \tag{3.37}$$

which is rewritten as

$$\frac{\epsilon_0 T'' + T'}{T} = \frac{X''}{X}. \tag{3.38}$$

As in the case of the classical equation, both sides of the equation are constant and, to avoid trivial solutions, we assume $\lambda = -\mu^2$. For instance, X is the solution to

$$\begin{cases} X'' + \mu^2 X = 0 & 0 < x < 1, \\ X(0) = X(1) = 0 \end{cases} \tag{3.39}$$

The solution to the problem above is a whole family of solutions given by

$$X_n(x) = \sin(\mu_n x), \tag{3.40}$$

where $\mu_n = \pi n$ and hence $\lambda_n = -\pi^2 n^2$. Up to here the method is identical to the one presented in the previous chapter. Let us now focus on the equation for T, given by

$$\epsilon_0 T'' + T' + \mu_n^2 T = 0. \tag{3.41}$$

To solve this ODE, let us consider the characteristic equation

$$\epsilon_0 r^2 + r + \mu_n^2 = 0, \tag{3.42}$$

whose roots are given by

$$r_1 = \frac{\sqrt{1-4\epsilon_0\mu_n^2}-1}{2\epsilon_0}, \; r_2 = -\frac{\sqrt{1-4\epsilon_0\mu_n^2}+1}{2\epsilon_0}. \tag{3.43}$$

Since $\mu_n \to \infty$, there exists a value $n_0 = n_0(\epsilon_0)$ such that the term $\Delta_n = 1 - 4\epsilon_0\mu_n^2$ changes its sign from positive to negative for $n > n_0$. Due to this bifurcation the character of the solution to (3.41) changes when crossing the value n_0. Moreover, the solution reads

$$T_n(t) = \begin{cases} A_n e^{\frac{\sqrt{\Delta_n}-1}{2\epsilon_0}t} + B_n e^{-\frac{\sqrt{\Delta_n}+1}{2\epsilon_0}t} & \text{if } n < n_0, \\ e^{-\frac{t}{2\epsilon_0}}\left[C_n \sin\left(\frac{\sqrt{-\Delta_n}}{2\epsilon_0}t\right) + D_n \cos\left(\frac{\sqrt{-\Delta_n}}{2\epsilon_0}t\right)\right] & \text{if } n > n_0. \end{cases} \tag{3.44}$$

Notice that it is exactly when $n > n_0$ that the solution displays a wavelike behaviour, whilst for $n < n_0$ the character of the solution is diffusive.

Hence, the solution to (3.41) is

$$u(x,t) = \sum_{n=1}^{\infty} T_n(t)\sin(\pi n x), \tag{3.45}$$

where we still have to impose the initial conditions to find the unknown coefficients of T_n. As in the previous chapter, these coefficients are computed using the initial conditions. Moreover, we consider the corresponding Fourier Series for each initial condition

$$\begin{aligned} f(x) &= \sum_{n=1}^{\infty} \bar{f}_n \sin(n\pi x), \\ g(x) &= \sum_{n=1}^{\infty} \bar{g}_n \sin(n\pi x), \end{aligned} \tag{3.46}$$

where

$$\bar{f}_n = 2\int_0^1 f(x)\sin(n\pi x)dx, \; \bar{g}_n = 2\int_0^1 g(x)\sin(n\pi x)dx. \tag{3.47}$$

Comparing each term of our solution and the initial conditions yields the expressions

$$\begin{aligned} A_n &= \frac{\sqrt{\Delta_n}+1}{2}\bar{f}_n + \frac{\epsilon_0}{\sqrt{\Delta_n}}\bar{g}_n, \\ B_n &= \frac{\sqrt{\Delta_n}-1}{2}\bar{f}_n - \frac{\epsilon_0}{\sqrt{\Delta_n}}\bar{g}_n, \\ C_n &= \frac{1}{\sqrt{-\Delta_n}}\left(2\epsilon_0\bar{g}_n + \bar{f}_n\right), \\ D_n &= \bar{f}_n. \end{aligned} \tag{3.48}$$

As an example, consider $f(x) = \sin(\pi x)$ and $g(x) = x(1-x)$ as the initial conditions to (3.35). Trivially one has

$$\bar{f}_n = \begin{cases} 1 & n = 1, \\ 0 & n > 1, \end{cases} \tag{3.49}$$

whilst

$$\bar{g}_n = 2\int_0^1 g(x)\sin(\pi n x)dx = \begin{cases} \dfrac{8}{\pi^3 n^3} & n \text{ odd}, \\ 0 & n \text{ even}. \end{cases} \tag{3.50}$$

Let us assume $\alpha = 10^{-7} m^2/s$, which is a typical value for the thermal diffusivity, and $L = 0.01m$. It follows $\epsilon_0 = 10^{-3}\tau_0$. Choosing, for instance, $\tau_0 = 10^{-5}s$ yields $\epsilon_0 = 10^{-8}$ and therefore

$$\Delta_n \geq 0 \Leftrightarrow n \leq \frac{1}{2\pi\sqrt{10^{-8}}} \sim 1591.55, \tag{3.51}$$

hence $n_0 = 1591$. Observe from this condition that as $\tau_0 \to 0$, the contribution of the part of T_n involving C_n and D_n decreases, and hence the wave character of the solution disappears. In fact, the first term involving these coefficients is of the order of 10^{-20}, and hence the wavelike character does not have much importance in this case. Observe that, in general, the value of n_0 depends also on the length

$$\Delta_n \geq 0 \Leftrightarrow n \leq \frac{L}{2\pi\sqrt{\alpha\tau_0}}. \tag{3.52}$$

From (3.52) it follows that the wave terms become more important as the length decreases. For instance, a decrease of one order of magnitude would of L reduces the threshold one order of magnitude, too.

To compare both models, let us consider (3.35) but taking the classical heat equation as the governing equation, i.e., consider

$$\begin{cases} u_t - u_{xx} = 0 & 0 < x < 1,\ t > 0, \\ u(x,0) = f(x) & 0 < x < 1, \\ u(0,t) = u(1,t) = 0 & t > 0, \end{cases} \tag{3.53}$$

where we have not taken into account the second initial condition since this problem does not involve a second derivative in time. The solution to this problem is

$$u^0(x,t) = e^{-\pi^2 t}\sin(\pi x), \tag{3.54}$$

which corresponds to the Fourier series

$$\sum_{n=1}^{\infty} \bar{f}_n e^{-n^2\pi^2 t}\sin(n\pi x). \tag{3.55}$$

where the coefficients $\bar{f}_n$ are defined in (3.49). Notice that, since $\lim\limits_{\epsilon_0\to 0}\Delta_n = 1$, it turns out that $A_n \to \bar{f}_n$ and $B_n \to 0$ as $\epsilon_0 \to 0$. On the other hand, as ϵ_0 decreases, and hence τ_0 decreases, we also have that n_0 grows and hence the impact of the wave-like part becomes weaker and weaker. Moreover we have that $n_0 \to \infty$. The question that remains is what happens to the terms $e^{(\sqrt{\Delta_n}-1)t/2\epsilon_0}$ as $\epsilon_0 \to 0$. Let us analyze the exponent

$$\frac{\sqrt{\Delta_n}-1}{2\epsilon_0}t = \frac{\sqrt{1-4\epsilon_0\mu_n^2}-1}{2\epsilon_0}t. \tag{3.56}$$

Recall that in the limit as $x \to 0$ one has

$$\sqrt{1-x} = 1 - \frac{x}{2} + O(x^2), \tag{3.57}$$

and therefore

$$\begin{aligned} \frac{\sqrt{1-4\epsilon_0\mu_n^2}-1}{2\epsilon_0}t &= \frac{1-\dfrac{4\epsilon_0\mu_n^2}{2}+O(\epsilon_0^2)-1}{2\epsilon_0} \\ &= \frac{-2\epsilon_0\mu_n^2 t + O(\epsilon_0^2)}{2\epsilon_0} \\ &= -\mu_n^2 t + O(\epsilon_0). \end{aligned} \tag{3.58}$$

Finally we obtain

$$\lim_{\epsilon_0 \to 0} e^{\frac{\sqrt{\Delta_n}-1}{2\epsilon_0}t} = e^{-\mu_n^2 t}. \tag{3.59}$$

These last observations prove that

$$\lim_{\epsilon_0 \to 0} u(x,t) = u^0(x,t). \tag{3.60}$$

Observe that the choice of the initial thermal velocity seems to be arbitrary, since its contribution disappears after taking the limit $\epsilon_0 \to 0$. In the next chapter we will give a result that relates the solutions to both problems in a more concrete way. Figure 3.2 shows that the behaviour of the solutions to the hyperbolic problem differs strongly from the solution to the classical model as ϵ_0 increases. If we focus on the behaviour of the solution for $\epsilon_0 = 1$ we see in figure 3.3 that the oscillations happen quickly, while figure 3.4 shows wavelike character of these oscillations. The lower the value of ϵ_0, the more the solution agrees with the solution to Fourier's model. In fact, the solution for $\epsilon = 10^{-7}$ seems to coincide in all four plots with the classical solution, although in a lower scale we would observe that they do not coincide. We also observe that there are strong oscillations in the temperature for larger values of ϵ_0. For instance, the solution for $\epsilon_0 = 1$ changes its sign twice in these plots. In practise, the value of the thermal diffusivity α is of the order of $10^{-7}m^2/s$, and the relaxation time can be of the order of picoseconds ($\sim 10^{-12}s$) in some cases. Thus $\epsilon_0 \ll 1$ in most situations, unless the spatial scale is of the order of $10^{-9}m$, i.e., if we were working in the nanoscale.

Eigenfunction expansion

This method is analogously applicable to the case of the classical heat equation. Consider (3.35) with a heat source of the form $S(x)$. We define u_{hom} as the solution to (3.35), and u_{source} as the solution to

$$\begin{cases} \epsilon_0 u_{tt} + u_t - u_{xx} = S & 0 < x < 1,\ t > 0, \\ u(x,0) = 0 & 0 < x < 1, \\ u_t(x,0) = 0 & 0 < x < 1, \\ u(0,t) = u(1,t) = 0 & t > 0. \end{cases} \tag{3.61}$$

Then, using the superposition principle, observe that $u := u_{hom} + u_{source}$ solves the complete nonhomogeneous problem

$$\begin{cases} \epsilon_0 u_{tt} + u_t - u_{xx} = S & 0 < x < 1,\ t > 0, \\ u(x,0) = f(x) & 0 < x < 1, \\ u_t(x,0) = g(x) & 0 < x < 1, \\ u(0,t) = u(1,t) = 0 & t > 0. \end{cases} \tag{3.62}$$

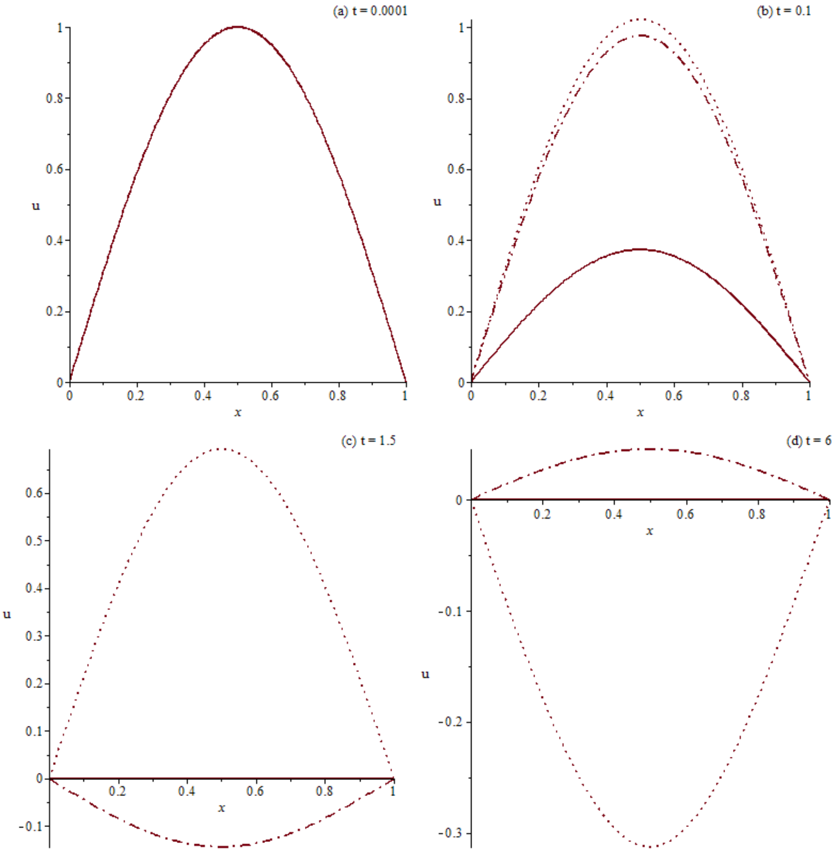

Figure 3.2: Plot of the temperature profiles for different values of t and $\epsilon_0 = 0$ (solid line), $\epsilon_0 = 10^{-5}$ (dashed line),$\epsilon_0 = 1$ (dashed-dotted line) and $\epsilon_0 = 16$ (dotted line). The graph for $\tau_0 = 0$ represents the solution to the classical problem.

Assuming that the solution to (3.61) admits an eigenfunction expansion of the form

$$u(x,t) = \sum_{n=1}^{\infty} a_n(t)\phi_n(x), \tag{3.63}$$

where ϕ_n are the eigenfunctions of the operator ∂_x^2, i.e., they satisfy

$$\phi_{xx} = -\mu^2\phi, \tag{3.64}$$

for a certain $\mu > 0$ (recall that the eigenvalues of the laplacian are of this form [1]). The boundary conditions in (3.61) imply $\phi(0) = \phi(1) = 0$ and hence

$$\phi_n(x) = \sin(n\pi x), \;\; \mu_n = n\pi. \tag{3.65}$$

Since the eigenfunctions are solutions to the Sturm-Liouville problem, they have an orthonormal basis [1] given by $\{2\sin(n\pi x)\}$, and we can expand S into

$$S(x) = \sum_{n=1}^{\infty} b_n \sin(n\pi x), \tag{3.66}$$

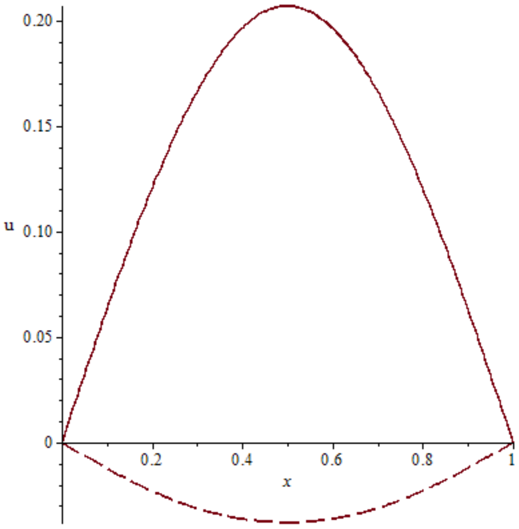

Figure 3.3: Solution for $\epsilon_0 = 1$ at $t = 0.5$ (solid line) and $t = 0.6$ (dashed line). The solution oscillates strongly.

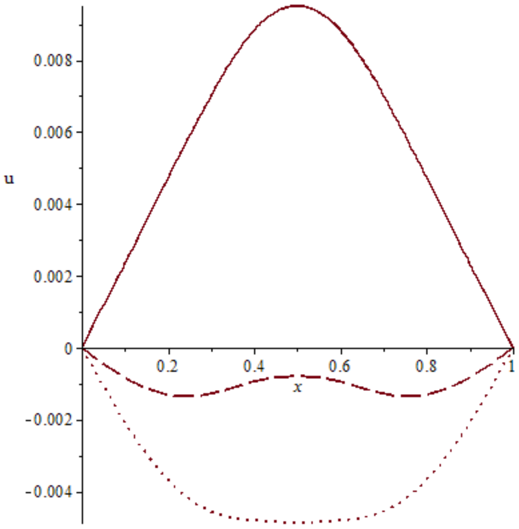

Figure 3.4: View of the wave-like character of the solution for $\epsilon_0 = 1$ at $t = 0.5838$ (solid line), $t = 0.5839$ (dashed line) and $t = 0.5840$ (dashed-dotted line).

where

$$b_n = 2\int_0^1 S(x)\sin(n\pi x)dx. \tag{3.67}$$

Substituting (3.63) and (3.67) into (3.61) we obtain, since we have a basis,

$$\begin{cases} \epsilon_0 a_n'' + a_n' + \mu_n^2 a_n = b_n, \\ a(0) = a'(0) = 0, \end{cases} \tag{3.68}$$

where we have derived the initial conditions from the initial conditions in (3.61). The solution is, after a similar study as in the previous section,

$$a_n(t) = \begin{cases} \frac{b_n}{\mu_n^2\sqrt{\Delta_n}}\left(\sqrt{\Delta_n} - e^{-t/2\epsilon_0}\sinh\left(\frac{\sqrt{\Delta_n}}{2\epsilon_0}t\right) - e^{-t/2\epsilon_0}\sqrt{\Delta_n}\cosh\left(\frac{\sqrt{\Delta_n}}{2\epsilon_0}t\right)\right) & \text{if } n < n_0, \\ \frac{b_n}{\mu_n^2\sqrt{-\Delta_n}}\left(\sqrt{-\Delta_n} - e^{-t/2\epsilon_0}\sin\left(\frac{\sqrt{-\Delta_n}}{2\epsilon_0}t\right) - e^{-t/2\epsilon_0}\sqrt{-\Delta_n}\cos\left(\frac{\sqrt{-\Delta_n}}{2\epsilon_0}t\right)\right) & \text{if } n > n_0. \end{cases} \tag{3.69}$$

Therefore we have that

$$u_{source}(x,t) = \sum_{n=1}^{\infty} a_n(t)\sin(n\pi x). \tag{3.70}$$

is the solution to (3.61).

If we take the limit as $\epsilon_0 \to 0$, we obtain, using the results of the previous study of the separation of variables,

$$\lim_{\epsilon_0 \to 0} a_n(t) = \frac{b_n}{\mu_n^2}\left(1 - e^{-\mu_n^2 t}\right) := a_n^0(t). \tag{3.71}$$

Observe that a_n^0 is the solution to

$$\begin{cases} a_n' + \mu_n^2 a_n = b_n, \\ a_n(0) = 0, \end{cases} \tag{3.72}$$

i.e., the limit equation of (3.68). It is straightforward to observe that $u^0(x,t) = \sum_{n=1}^{\infty} a_n^0(t)\sin(n\pi x)$ is the solution to

$$\begin{cases} u_t - u_{xx} = S & 0 < x < 1,\ t > 0, \\ u(x,0) = 0 & 0 < x < 1, \\ u(0,t) = u(1,t) = 0 & t > 0, \end{cases} \tag{3.73}$$

i.e., the limit problem of (3.61). Therefore, as in the previous case we obtain

$$\lim_{\epsilon_0 \to 0} u(x,t) = u^0(x,t). \tag{3.74}$$

Duhamel's method

Assume now that the heat source in (3.61) depends also on time such that $S(x,t) = S_1(x)S_2(t)$. In this case we can use Duhamel's method, which consists in introducing an auxiliary parameter s and solving

$$\begin{cases} \epsilon_0 u_{tt} + u_t - u_{xx} = 0 & 0 < x < 1,\ t > s, \\ u(x,s;s) = 0 & 0 < x < 1, \\ u_t(x,s;s) = S_1(x)S_2(s) & 0 < x < 1, \\ u(0,t;s) = u(1,t;s) = 0 & t > s. \end{cases} \tag{3.75}$$

If we let $w(x,t;s)$ be the solution to this problem, it follows by theorem 3 that $\int_0^t w(x,t;s)ds$ is the solution to

$$\begin{cases} \epsilon_0 u_{tt} + u_t - u_{xx} = S & 0 < x < 1,\ t > 0, \\ u(x,0) = 0 & 0 < x < 1, \\ u_t(x,0) = 0 & 0 < x < 1, \\ u(0,t) = u(1,t) = 0 & t > 0. \end{cases} \tag{3.76}$$

w using the eigenfunction expansion provided above. In this case, the equations for a_n are

$$\begin{cases} \epsilon_0 a_n'' + a_n' + \mu_n^2 a_n = 0, \\ a_n(s) = 0, \\ a_n'(s) = c_n S_2(s), \end{cases} \tag{3.77}$$

where the coefficients c_n are the coefficients of the expansion of $S_1(x)$, i.e.,

$$c_n = 2\int_0^1 S_1(x)\sin(n\pi x)dx. \tag{3.78}$$

The expression a_n in this case is

$$a_n(t;s) = \begin{cases} \frac{2c_n\epsilon_0}{\sqrt{\Delta_n}} e^{-\frac{t-s}{2\epsilon_0}(t-s)} \sinh\left(\frac{\sqrt{\Delta_n}}{2\epsilon_0}(t-s)\right) S_2(s) & \text{if } n < n_0, \\ \frac{2c_n\epsilon_0}{\sqrt{-\Delta_n}} e^{-\frac{t-s}{2\epsilon_0}(t-s)} \sin\left(\frac{\sqrt{-\Delta_n}}{2\epsilon_0}(t-s)\right) S_2(s) & \text{if } n > n_0. \end{cases} \tag{3.79}$$

Using these we finally have that the solution to (3.76) is

$$u(x,t) = \sum_{n=1}^{\infty} \int_0^t a_n(t;s)ds \sin(n\pi x). \tag{3.80}$$

Notice that the boundary conditions are implicitly present in the terms a_n, since they contain the Fourier coefficients of the spatial part of the heat source. We will use this method in an explicit example in further sections. Observe also that if no force is involved in the problem, then $a_n \equiv 0$ for all n and hence $u_{source} \equiv 0$, no matter if we use the eigenfunction expansion or Duhamel's method. We will later adapt the latter also for problems involving the classical heat equation.

Contrary to the case of the previous approximate methods, this technique is not compatible with taking the limit $\epsilon_0 \to 0$, in the sense that we do not obtain the solution of the limiting classical heat equation. Making a similar study as in the separation of variables, we obtain

$$\lim_{\epsilon_0 \to 0} a_n(t;s) = 0, \tag{3.81}$$

and hence

$$\lim_{\epsilon_0 \to 0} u(x,t) = 0. \tag{3.82}$$

On the other hand, consider the limit problem

$$\begin{cases} u_t - u_{xx} = S & 0 < x < 1,\ t > 0, \\ u(x,0) = 0 & 0 < x < 1, \\ u(0,t) = u(1,t) = 0 & t > 0. \end{cases} \tag{3.83}$$

Trivially $w \equiv 0$ is not a solution of (3.84) since it does not satisfy the equation if $S_1 S_2 \neq 0$. The problem relies on the auxiliary problem (3.75), which in the limit is

$$\begin{cases} u_t - u_{xx} = 0 & 0 < x < 1,\ t > 0, \\ u(x, s; s) = 0 & 0 < x < 1, \\ u(0, t; s) = u(1, t; s) = 0 & t > s. \end{cases} \tag{3.84}$$

Exact solution methods. Fourier Transforms

Definition 5 (Fourier Transform on L^1)**.** Let $f \in L^1(\mathbb{R}^n)$, we define its *Fourier transform*

$$\mathcal{F}_x\{f\}(y) = \hat{f}(y) := \frac{1}{(2n)^{n/2}} \int_{\mathbb{R}^n} e^{-ixy} f(x) dx, \tag{3.85}$$

and its *inverse Fourier transform* as

$$\mathcal{F}_x^{-1}\{f\}(y) = \check{f}(y) := \frac{1}{(2n)^{n/2}} \int_{\mathbb{R}^n} e^{ixy} f(x) dx, \tag{3.86}$$

where $y \in \mathbb{R}^n$. Since $|e^{\pm ixy}| = 1\ \forall x, y \in \mathbb{R}^n$ and $f \in L^1(\mathbb{R}^n)$, both integrals converge and $\hat{f}, \check{f} \in L^1(\mathbb{R}^n)$.

The definition of Fourier transform also applies in $L^2(\mathbb{R}^n)$, as is given in [2]. We use this transform to solve (3.4) on an infinite domain without any heat source, i.e. we consider

$$\begin{cases} \tau_0 T_{tt} + T_t - \alpha T_{xx} = 0, & x \in \mathbb{R},\ t > 0 \\ T(x, 0) = f(x), & x \in \mathbb{R}, \\ T_t(x, 0) = g(x), & x \in \mathbb{R}. \end{cases} \tag{3.87}$$

For the nondimensional variables choose now $\gamma_x = 2\alpha/c$, $\gamma_t = 2\tau_0$ in (2.10), whilst

$$u' = \frac{T}{T_0}, \tag{3.88}$$

where T_0 is a reference value for the temperature. The dimensionless equation is

$$u_{tt} + 2u_t - u_{xx} = 0, \tag{3.89}$$

where we have dropped again the primes for simplicity. Notice that in this form, the parameter τ_0 disappears from the equation, but not from the problem since it is still present in the definition of the variables. Hence, using these variables we will not have to distinguish cases while solving the equation. Recall that in the case of the separation of variables method we have made the distinction to see the importance of the diffusive and wavelike components of the solution.

Equation (3.89) is known as the *telegraph equation*, where physically the term $2u_t$ represents the damping of a wave that is being propagated.

Applying the Fourier transform to (3.89) yields

$$\begin{cases} \hat{u}_{tt} + \hat{u}_t + y^2 \hat{u} = 0, & t > 0, \\ \hat{u} = \hat{f},\ \hat{u}_t = \hat{g} & t = 0. \end{cases} \tag{3.90}$$

We seek a solution of the form $\hat{u} = ae^{bt}$ for $a, b \in \mathbb{C}$. Substituting this expression into (3.90) we obtain

$$b^2\hat{u} + 2b\hat{u} + y^2\hat{u} = 0, \tag{3.91}$$

which satisfies the characteristic equation

$$b^2 + 2b + y^2 = 0, \tag{3.92}$$

from where we deduce

$$b = -1 \pm \sqrt{1 - y^2}. \tag{3.93}$$

Therefore the solution for $\hat{u}$ is of the form

$$\hat{u}(y,t) = \begin{cases} e^{-t}\left(a_1(y)e^{\sqrt{\Delta(y)}t} + a_2(y)e^{-\sqrt{\Delta(y)}t}\right) & \text{if } |y| < 1, \\ e^{-t}\left(a_1(y)e^{i\sqrt{-\Delta(y)}t} + a_2(y)e^{-i\sqrt{-\Delta(y)}t}\right) & \text{if } |y| \geq 1, \end{cases} \tag{3.94}$$

where $\Delta(y) = 1 - y^2$ and a_1, a_2 are chosen to satisfy the initial conditions

$$\hat{u} = \hat{f},\ \hat{u}_t = \hat{g}. \tag{3.95}$$

That is, $a_1(y)$ and $a_2(y)$ have to be chosen such that

$$\hat{f}(y) = a_1(y) + a_2(y), \tag{3.96}$$

and

$$\hat{g}(y) = \begin{cases} a_1(y)(\sqrt{\Delta(y)} - 1) - a_2(y)(\sqrt{\Delta(y)} + 1) & \text{if } |y| < 1, \\ a_1(y)(i\sqrt{-\Delta(y)} - 1) - a_2(y)(-i\sqrt{-\Delta(y)} + 1) & \text{if } |y| \geq 1. \end{cases} \tag{3.97}$$

Then, using (3.86) we recover the solution to the initial problem

$$\begin{aligned} u(x,t) = \ & \frac{e^{-t}}{\sqrt{2\pi}}\int_{\{|y|<1\}} a_1(y)e^{ixy+\sqrt{\Delta(y)}t} + a_2(y)e^{ixy-\sqrt{\Delta(y)}t}dy \\ & + \frac{e^{-t}}{\sqrt{2\pi}}\int_{\{|y|\geq 1\}} a_1(y)e^{i(xy+\sqrt{-\Delta(y)}t)} + a_2(y)e^{i(xy-\sqrt{-\Delta(y)}t)}dy. \end{aligned} \tag{3.98}$$

Let us, for instance, choose f such that $\hat{f}(y) = H(1 - |y|)$ and let $g(x) = 0$. Using (3.86) yields $f(x) = 2\sin(x)/x$. It is straightforward to obtain $\hat{g}(y) = 0$ and hence, using (3.96) and (3.97) we obtain

$$\begin{aligned} a_1(y) &= \begin{cases} \dfrac{\sqrt{\Delta(y)} + 1}{2\sqrt{\Delta(y)}} & \text{if } |y| < 1, \\ 0 & \text{if } |y| \geq 1, \end{cases} \\ a_2(y) &= \begin{cases} \dfrac{\sqrt{\Delta(y)} - 1}{2\sqrt{\Delta(y)}} & \text{if } |y| < 1, \\ 0 & \text{if } |y| \geq 1. \end{cases} \end{aligned} \tag{3.99}$$

Therefore, the solution to the initial value problem is given by

$$u(x,t) = \frac{e^{-t}}{\sqrt{2\pi}}\int_{-1}^{1} a_1(y)e^{ixy+\sqrt{\Delta(y)}t} + a_2(y)e^{ixy-\sqrt{\Delta(y)}t}dy. \tag{3.100}$$

Using the fact that

$$\int_{-1}^{0} e^{ixy}dy = \int_{0}^{1} e^{-ixy}dy, \tag{3.101}$$

we can rewrite u as

$$u(x,t) = \frac{e^{-t}}{\sqrt{2\pi}} \int_0^1 2a_1(y)e^{\sqrt{\Delta(y)}t}\cos(xy) + 2a_2(y)e^{-\sqrt{\Delta(y)}t}\cos(xy)dy \tag{3.102}$$

We observe from figure 3.5 that the example used is not particularly interesting in our context, since the wave-like character is a consequence of the the initial condition $u(x,0) = f(x)$ more so than the properties of the equation.

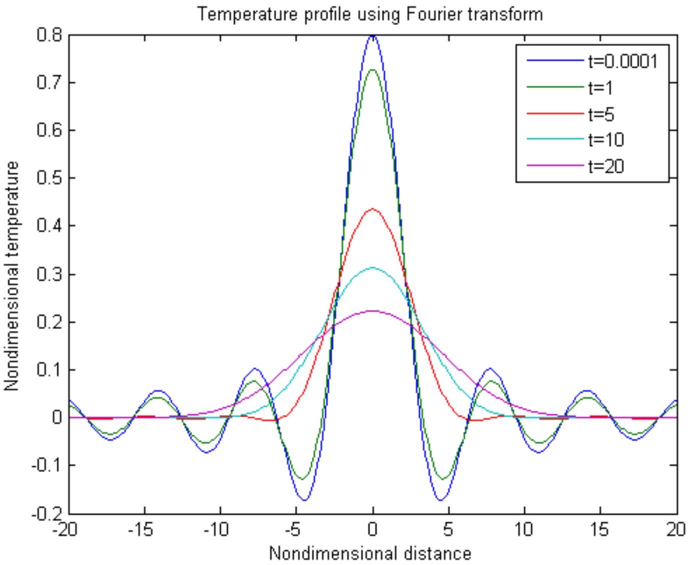

Figure 3.5: Solution to (3.87) for different values of nondimensional time.

Other authors, such as Chen [15], have solved other problems involving the hyperbolic heat equation using the Laplace transform introduced in chapter 2, but we will not go into further details regarding this method since the computation of the inverse transform is quite difficult.

In fact, Cattaneo [5] showed via Laplace and Fourier transforms that the exact solution to (3.89) is

$$u(x,t) = \frac{e^{-t}}{2}\left(F(x+t) + F(x-t) + \int_{x-t}^{x+t} I(s,x,t)ds\right), \tag{3.103}$$

where

$$\begin{aligned} I(s,x,t) = \;& (G(s)+F(s))\,J_0\left(\sqrt{(s-x)^2-t^2}\right) \\ & -2tF(s)J_0'\left(\sqrt{(s-x)^2-t^2}\right). \end{aligned} \tag{3.104}$$

The functions F and G are the corresponding initial conditions in (3.87) after applying the nondimensional variables, while J_0 refers to the Bessel function of zeroth order. In particular, we observe that if the initial conditions have compact support, then u does also have compact support, i.e. the speed of heat propagation is finite.

4

Limit behaviour of HHE-solutions

The aim of this section is to discuss the connection between the solutions to the models of Fourier and Maxwell-Cattaneo. Moreover we will highlight a result due to Nagy, Ortiz and Reula [16], which, under certain circumstances, relates the solutions to both models under certain conditions on the initial conditions, and how fast the hyperbolic solution tends to the classical one. After giving the proof of this theorem, we will prove an own result that will give other conditions to justify this convergence from the HHE-solution to its certain CHE-solution.

4.1 The Nagy-Ortiz-Reula Theorem

Let us reduce the model to one spatial dimension for simplicity, and let us consider periodic boundary conditions. That is, take the interval $[0, L]$ and identify its endpoints, and consider conditions of the form

$$\partial_x^i T(0,t) = \partial_x^i T(L,t) \ \forall t > 0, \tag{4.1}$$

where $i = 0, 1$. Let us consider, without an external heat source, the pair of equations (1.1) and (3.1) of the Maxwell-Cattaneo model, i.e. consider the system

$$\begin{cases} c_p \rho T_t + q_x = 0, \\ \tau_0 q_t + q = -k T_x. \end{cases} \tag{4.2}$$

If we now consider the new variables

$$u = T, \ v = -\frac{q}{c_p \rho}, \tag{4.3}$$

we obtain the coupled system of equations

$$\begin{cases} u_t = v_x, \\ \epsilon^2 v_t = u_x - \dfrac{1}{\alpha} v, \end{cases} \tag{4.4}$$

where $\epsilon = c^{-1} = \sqrt{\tau_0/\alpha}$ is the inverse of the second sound and $\alpha = k/(c_p\rho)$ is again the thermal diffusivity. Since ϵ^2 is proportional to τ_0, they are equivalent parameters. Notice that if we eliminate v from the system we recover the hyperbolic heat equation.

One of the fundamental differences between the two models we are considering is that we only need one initial condition for the classical model while we need two conditions for the hyperbolic one. We set the intial conditions for (4.4) to be $u(x,0) = f(x)$ and $v(x,0) = g(x)$. For instance, let u^0 be the solution to the problem

$$\begin{cases} u^0_t - \alpha u^0_{xx} = 0, \\ u^0(x,0) = f(x) + \alpha\epsilon^2\Delta_x, \end{cases} \tag{4.5}$$

where $\Delta = g - \alpha f_x$. Thus, we consider similar initial conditions for both models, at least up to order ϵ^2. Under these circumstances, the following theorem by Nagy *et al.* [16] relates the solutions to the hyperbolic model to the parabolic solution u^0.

Theorem 5. *Let $f \in C^{n+2}(S^1)$ and $g \in C^{n+1}(S^1)$ be the initial data for the systems (4.4) and (4.5) with $n \geq 2$. Then the corresponding solutions (u, v) and u^0 are related as follows:*

$$\begin{aligned} u &= u^0 - \alpha\epsilon^2\Delta_x e^{-t/\alpha\epsilon^2} + u^R, \\ v &= \alpha u^0_x + \Delta e^{-t/\alpha\epsilon^2} + v^R, \end{aligned} \tag{4.6}$$

for certain functions u^R, v^R. Furthermore, one has that the Sobolev norms of u^R and v^R can be bounded for all $t \geq 0$ in terms of the initial data as follows:

$$\|u^R\|^2_{H^m} + \epsilon^2\|v^R\|^2_{H^m} \leq \epsilon^4\alpha^4\left(\|f_{xx}\|^2_{H^m} + \frac{3\epsilon^2}{2}\|\Delta_{xx}\|^2_{H^m} + \|\Delta_{xxx}\|^2_{H^m}\right), \tag{4.7}$$

with $0 \leq m \leq n-2$.

Proof. It is always possible to define the solution to (4.4) as in (4.6). The unknown functions u^R, v^R then have to satisfy the problem

$$\begin{cases} u^R_t = v^R_x, \\ \epsilon^2 v^R_t = u^R_x - \frac{1}{\alpha}v^R + \epsilon^2\sigma, \end{cases} \tag{4.8}$$

where $\sigma = -\alpha\left(\Delta_{xx}e^{-t/\alpha\epsilon^2} + u^0_{xt}\right)$. From the initial conditions $u(x,0) = f(x)$ and $v(x,0) = g(x)$ it follows that $u^R(x,0) = 0$ and $v^R(x,0) = -\epsilon^2\alpha^2\Delta_{xx}$. Let us now define the following energy functional for the couple (u^R, v^R),

$$E_R = \int_0^L (u^R)^2 + \epsilon^2(v^R)^2 dx = \|u^R\|^2_{L^2} + \epsilon^2\|v^R\|^2_{L^2}, \tag{4.9}$$

with the time derivative

$$E'_R = 2\int_0^L \left(u^R_t u^R + \epsilon^2 v^R_t v^R\right) dx. \tag{4.10}$$

Using (4.8) it follows that

$$E'_R = 2\int_0^L \left(u^R v^R_x + v^R u^R_x - \frac{1}{\alpha}(v^R)^2 + \epsilon^2\sigma v^R\right) dx, \tag{4.11}$$

and, since we are identifying $x = 0$ and $x = L$, the two first terms cancel each other out using integration by parts. Completing squares we obtain

$$E'_R = 2\int_0^L \left[\frac{\alpha}{4}\epsilon^4\sigma^2 - \left(\frac{v^R}{\sqrt{\alpha}} - \epsilon^2\sigma\frac{\sqrt{\alpha}}{2}\right)^2\right] dx \leq \frac{\alpha\epsilon^4}{2}\int_0^L \sigma^2 dx. \tag{4.12}$$

Thus, integrating the inequality,

$$E_R(t) \leq E_R(0) + \frac{\alpha\epsilon^4}{2}\int_0^t \|\sigma\|_{L^2}^2 ds. \tag{4.13}$$

Now, using the initial data we obtain $E_R(0) = \epsilon^6\alpha^4\|\Delta_{xx}\|_{L^2}^2$, and hence

$$E_R(t) \leq \epsilon^6\alpha^4\|\Delta_{xx}\|_{L^2}^2 + \frac{\alpha\epsilon^4}{2}\int_0^t \|\sigma\|_{L^2}^2 ds. \tag{4.14}$$

Let us now bound the term involving σ. If we express σ in terms of the initial data and u^0 we obtain

$$\begin{array}{ll} \frac{\alpha\epsilon^4}{2}\int_0^t \|\sigma\|_{L^2}^2 ds & = \frac{\alpha\epsilon^4}{2}\int_0^t \|\sigma\|_{L^2}^2 ds \\ & = \frac{\alpha^3\epsilon^4}{2}\int_0^t\int_0^L \left(\Delta_{xx}e^{-s/\alpha\epsilon^2} + u^0_{xs}\right)^2 dxds \\ & \leq \alpha^3\epsilon^4\int_0^t\int_0^L \left[(\Delta_{xx})^2 e^{-2s/\alpha\epsilon^2} + (u^0_{xs})^2\right] dxds, \end{array} \tag{4.15}$$

where we have used the property $(a+b)^2 \leq 2(a^2+b^2)$. Notice that Δ does not depend on time, and hence computing the time integral of the first term is straightforward. We obtain

$$\begin{array}{ll} \int_0^t\int_0^L (\Delta_{xx})^2 e^{-2s/\alpha\epsilon^2} dxds & = \frac{\alpha\epsilon^2}{2}\int_0^L (1 - e^{-2t/\alpha\epsilon^2})\Delta_{xx}^2 dx \\ & \leq \frac{\alpha\epsilon^2}{2}\int_0^L \Delta_{xx}^2 dx \\ & = \frac{\alpha\epsilon^2}{2}\|\Delta_{xx}\|_{L^2}^2. \end{array} \tag{4.16}$$

In order to deal with the term of (4.15) involving u^0 we will use the limiting problem that this function solves. Therefore we have, assuming again that $x = 0$ and $x = L$ are identified and therefore boundary terms vanish,

$$\begin{array}{ll} \int_0^t\int_0^L (u^0_{xs})^2 dxds & = \alpha\int_0^t\int_0^L (u^0_{xs})(u^0_{xxx}) dxds \\ & = -\alpha\int_0^t\int_0^L (u^0_{sxx})(u^0_{xx}) dxds \\ & = \frac{\alpha}{2}\int_0^L \left.(u^0_{xx})^2\right|_{s=0} - \left.(u^0_{xx})^2\right|_{s=t} dx \\ & \leq \frac{\alpha}{2}\int_0^L \left.(u^0_{xx})^2\right|_{s=0} dx \\ & = \frac{\alpha}{2}\int_0^L (f_{xx} + \alpha\epsilon^2\Delta_{xxx})^2 dx \\ & \leq \alpha\|f_{xx}\|_{L^2}^2 + \alpha^3\epsilon^4\|\Delta_{xxx}\|_{L^2}^2. \end{array} \tag{4.17}$$

If we now substitute (4.16) and (4.17) into (4.15) we finally obtain, combining (4.15) and (4.14),

$$E_R(t) \leq \epsilon^4\alpha^4\left(\frac{3\epsilon^2}{2}\|\Delta_{xx}\|_{L^2}^2 + \|f_{xx}\|_{L^2}^2 + \epsilon^4\alpha^2\|\Delta_{xxx}\|_{L^2}^2\right). \tag{4.18}$$

Notice that we have proved the statement of the theorem only for $m = 0$. However, taking energy functionals of the form

$$E_R^{(i)} = \|\partial_x^i u^R\|_{L^2}^2 + \epsilon^2\|\partial_x^i v^R\|_{L^2}^2, \tag{4.19}$$

we obtain the same inquality as in (4.18) but with all the involved functions differentiated with respect to x. This happens because the equations in (4.8) are linear with respect to the spatial variable. By adding this inequalities we obtain (4.7) for all H^m-norms, assuming that the initial data is differentiable enough. If $f \in C^{n+2}(S^1)$ and $g \in C^{n+1}$, then the statement is true for $m \leq n-2$, since we then can assure that the right hand side of (4.7) is finite.

□

An easy example is given by taking $f \equiv 1$ and $g \equiv 0$. In this case, the solution to (4.5) is trivially $u^0 \equiv 1$. Assuming no initial heat flux and a constant initial temperature, it is easy to show that the solution to (4.4) is also trivial, given by $u \equiv 1$ and $v \equiv 0$. Using the previous theorem, we have that $\Delta \equiv 0$ and hence the bound on u^R and v^R is zero, which leads to $u^R \equiv v^R \equiv 0$, thus the theorem holds.

A direct consequence of theorem 5 is that u converges uniformly to the limit solution u^0[16]. Using the theorem one has

$$\begin{aligned} |u-u^0| &= |u^R - \alpha\epsilon\Delta_x e^{-t/\alpha\epsilon^2}| \\ &\leq |u^R| + \alpha\epsilon|\Delta_x| e^{-t/\alpha\epsilon^2} \\ &\leq \|u^R\|_{H^m} + \alpha\epsilon\|\Delta_x\|_{H^m} e^{-t/\alpha\epsilon^2} \\ &\leq \sqrt{E_R} + \alpha\epsilon\|\Delta_x\|_{H^m} e^{-t/\alpha\epsilon^2} \\ &\leq \epsilon^2\alpha\left[\alpha\left(\|f_{xx}\|^2_{H^m} + \frac{3\epsilon^2}{2}\|\Delta_{xx}\|^2_{H^m} + \|\Delta_{xxx}\|^2_{H^m}\right)^{1/2} + \|\Delta_x\|_{H^m} e^{-t/\alpha\epsilon^2}\right]. \end{aligned} \tag{4.20}$$

We have now seen that under certain circumstances, the solution to Cattaneo's formulation tends to Fourier's solution as the speed c increases. Returning to the hyperbolic heat equation by eliminating v from (4.4), i.e.,

$$\epsilon^2 u_{tt} + \frac{1}{\alpha}u_t - u_{xx} = 0 \tag{4.21}$$

we can also relate the solution of this equation to the solution u^0 of (4.5). The condition on $u_t(x,0)$ follows from $u_t = v_x$ and is given by

$$u_t(x,0) = g_x(x). \tag{4.22}$$

Under these conditions we can also ensure that $u \to u^0$ uniformly when $\epsilon \to 0$.

4.2 Modified Nagy-Ortiz-Reula Theorem

Let us recall now the example of section 3.6, i.e, consider the two problems

$$\left\{\begin{array}{ll} \epsilon_0 u_{tt} + u_t - u_{xx} = 0 & 0 < x < 1,\ t > 0, \\ u(x,0) = \sin(\pi x)) & 0 < x < 1, \\ u_t(x,0) = x(1-x) & 0 < x < 1, \\ u(0,t) = u(1,t) = 0 & t > 0, \end{array}\right. \tag{4.23}$$

and

$$\left\{\begin{array}{ll} u_t - u_{xx} = 0 & 0 < x < 1,\ t > 0, \\ u(x,0) = \sin(\pi x)) & 0 < x < 1, \\ u(0,t) = u(1,t) = 0 & t > 0. \end{array}\right. \tag{4.24}$$

Let $u(x,t)$ and $u^0(x,t)$ be the solutions to the hyperbolic and the classical problems respectively. In section 3.6 we have already deduced that $u \to u^0$ as $\epsilon_0 \to 0$, fact that could not have been guaranteed by theorem 5. Therefore, let us prove a result that will justify it. The following theorem has not been taken from literature but has been deduced and proved to justify the example above and extrapolate it to other situations in a rigorous way.

Consider the space $C_0^n(0,L) = \{f \in C^n(0,L) : f(0) = f(L) = 0\}$, and notice that this space fits into our example.

Theorem 6. *Let $f \in C_0^2(0,L) \cap H^2(0,L)$ and $g \in H^1(0,L)$ be the initial data for the systems*

$$\begin{cases} u_t = v_x, \\ \epsilon^2 v_t = u_x - \frac{1}{\alpha} v, \\ u(x,0) = f(x), \; v(x,0) = g(x), \\ u(0,t) = u(L,t) = 0 \end{cases} \tag{4.25}$$

and

$$\begin{cases} u_t^0 - \alpha u_{xx}^0 = 0, \\ u^0(x,0) = f(x), \\ u^0(0,t) = u(L,t) = 0. \end{cases} \tag{4.26}$$

Moreover, assume that $u^0 \in C_0^{n+2}(0,L)$ for any $t > 0$, then the corresponding solutions (u,v) and u^0 are related as follows:

$$\begin{aligned} u &= u^0 + u^R, \\ v &= \alpha u_x^0 + v^R, \end{aligned} \tag{4.27}$$

for certain functions u^R, v^R. Furthermore, one has that the L^2-norms of u^R and v^R can be bounded for all $t \geq 0$ in terms of the initial data as follows:

$$\|u^R\|_{L^2}^2 + \epsilon^2 \|v^R\|_{L^2}^2 \leq \epsilon^2 \left(\|g\|_{L^2}^2 + \alpha^2 \|f_x\|_{L^2}^2 + \frac{\alpha^4 \epsilon^2}{2} \|f_{xx}\|_{L^2}^2 \right). \tag{4.28}$$

Proof. The proof is analogous to the proof in theorem 5. It is always possible to express the couple (u,v) as in (4.27). The couple $\left(u^R, v^R\right)$ satisfy the equations

$$\begin{cases} u_t^R = v_x^R, \\ \epsilon^2 v_t^R = u_x^R - \dfrac{1}{\alpha} v^R - \alpha \epsilon^2 u_{xt}^0. \end{cases} \tag{4.29}$$

If we now define E_R as in (4.9) and compute its time derivative, we obtain

$$E_R' = 2 \int_0^L \left(u^R v_x^R + v^R u_x^R - \frac{1}{\alpha} v^R - \alpha \epsilon^2 v^R u_{xt}^0 \right) dx. \tag{4.30}$$

Using now that $u(0,t) = u(L,t) = 0$, the two first terms vanish using integration by parts, and hence we obtain

$$\begin{aligned} E_R' &= 2 \int_0^L \left(-\frac{1}{\alpha} v^R - \alpha \epsilon^2 v^R u_{xt}^0 \right) dx \\ &= \frac{2}{\alpha} \int_0^L \left[\frac{\alpha^4 \epsilon^4}{4} \left(u_{xt}^0\right)^2 - \left(v^R + \frac{\alpha^2 \epsilon^2}{2} u_{xt}^0 \right)^2 \right] dx \\ &\leq \frac{2}{\alpha} \int_0^L \frac{\alpha^4 \epsilon^4}{4} \left(u_{xt}^0\right)^2 dx. \end{aligned} \tag{4.31}$$

Inspection of the original initial conditions yields $u^R(x,0)=0$ and $v^R(x,0)=g(x)-\alpha f_x(x)$, and hence, integrating the inequality above we obtain

$$\begin{aligned} E_R &\leq E(0)+\frac{2}{\alpha}\int_0^L \frac{\alpha^4\epsilon^4}{4}\left(u^0_{xt}\right)^2 dx \\ &\leq \epsilon^2\|g-\alpha f_x\|^2_{L^2}+\frac{\alpha^3\epsilon^4}{2}\int_0^L \left(u^0_{xt}\right)^2 dx. \end{aligned} \tag{4.32}$$

Using $u^0\in C_0^{n+2}(0,L)$ in the spatial variable, we obtain $u^0_{xx}\in C_0^n(0,L)$, and hence we can do the same procedure as in (4.17) to obtain

$$\int_0^L \left(u^0_{xt}\right)^2 dx \leq \alpha\|f_{xx}\|^2_{L^2}, \tag{4.33}$$

and hence we obtain the final result

$$E_R \leq \epsilon^2\left(\|g\|^2_{L^2}+\alpha^2\|f_x\|^2_{L^2}+\frac{\alpha^2\epsilon^2}{2}\|f_{xx}\|^2_{L^2}\right). \tag{4.34}$$

□

Notice that the proof does not require any special condition on g, except $g\in L^2(0,L)$. Let us explain why we require $g\in H^1(0,L)$. Recall that from (4.25) we can obtain the hyperbolic equation for u

$$\epsilon^2 u_{tt}+\frac{1}{\alpha}u_t-u_{xx}=0 \tag{4.35}$$

but where the second initial condition now reads $u_t(x,0)=g_x(x)$, and therefore we need this derivative to exist in order to have a well-defined initial value problem. In our example we have $\alpha=L=1$, $f(x)=\sin(\pi x)$ and $g_x(x)=x(1-x)$, hence we can set $g(x)=\frac{1}{2}x^2+\frac{1}{3}x^3$. From theorem 6 we also obtain a bound for the error $\|u-u^0\|_{L^2}$ directly from (4.28)

$$\begin{aligned} \|u-u^0\|^2_{L^2} &= \|u^R\|^2_{L^2}\leq E_R \\ &= \epsilon^2\left(\|g\|^2_{L^2}+\|f_x\|^2_{L^2}+\frac{\epsilon^2}{2}\|f_{xx}\|^2_{L^2}\right) \\ &\approx 5.06\epsilon^2+24.35\epsilon^4. \end{aligned} \tag{4.36}$$

4.3 Conclusions

Theorem 6 does not give enough information about the behaviour of v^R, since from (4.28) we only obtain, in the limit $\epsilon\to 0$,

$$\|v^R\|^2_{L^2}\leq \|g\|^2_{L^2}+\alpha^2\|f_x\|^2_{L^2}, \tag{4.37}$$

and hence in principle it could be possible that $\lim\limits_{\epsilon\to 0} v$ does not coincide with the heat flux given by Fourier's law. In fact, not even assuming a zero initial thermal velocity assures that the heat flux given by Cattaneo's model will tend to the one predicted by Fourier. Our modification of the N.O.R. theorem thus has to be reviewed and corrected, since the approximation for the heat flux cannot be controlled by the parameter ϵ by now.

It has been proved that given any arbitrary initial conditions for the hyperbolic system, the solution to the classical heat equation with the same initial temperature profile, up to order ϵ^2, remains near the hyperbolic solution for $t \geq 0$ if vanishing Dirichlet conditions or periodic boundary conditions are considered. Moreover, the HHE-solution tends to the CHE-solution as $\epsilon \to 0$. The HHE-solution can thus be approximated by the latter provided $\epsilon \ll 1$. The initial thermal velocity affects this approximation only for small values of t, according to (4.6).

5

Laser heating of a thin film

The use of heat sources such as lasers or microwaves has become more and more frequent in applications related to material processing, such as for example welding and drilling of metals or surface annealing [18]. Since these processes usually involve short laser pulses or high frequencies, the model by Fourier might give inaccurate predictions. In particular, if the duration of the laser pulse approaches the relaxation time, radiation absorption mechanisms become more and more important [17]. In this chapter we will study a simple example of laser radiation by considering a thin film heated symetrically on both sides for a short period of time. We will discuss four theoretical models to describe the heat transfer.

We consider a film of thickness L and with an initial temperature T_0 that is heated for a certain time t_0 due to the impact of a laser source on both sides of the film. Furthermore, assume that there is no heat transport in the orthogonal direction to the beam, hence that the problem is one-dimensional.

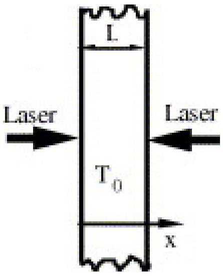

Figure 5.1: Physical configuration.

5.1 Model with Dirichlet boundary conditions

In a first attempt, let us think about the laser source as a fixed temperature at the boundaries for $t < t_0$, while it decreases in an unknown way for $t > t_0$. Then the equations for this model are

$$\begin{cases} T_t - \alpha T_{xx} = 0 & 0 < x < L, \ t > 0, \\ T(x,0) = T_0 & 0 < x < L, \\ T(0,t) = T(L,t) = T_w & t < t_0, \\ T(0,t) = T(L,t) = f(t) & t > t_0, \end{cases} \tag{5.1}$$

where f is an unknown function such that $f'(t) < 0$ for all $t > t_0$, and $T_w \gg T_0$. Let us focus only on the case $t < t_0$, that is, when the laser is contact with the boundary of the film. To reduce the number of parameters, let us apply the nondimensional variables (2.10) with $\gamma_x = L$, $\gamma_t = L^2/\alpha$ and $\gamma_T = T_w - T_0$. The parameter t_0 is scaled in the same manner as t. The resulting system is, after dropping the primes

$$\begin{cases} u_t - u_{xx} = 0 & 0 < x < 1, \ 0 < t < t_0, \\ u(x,0) = 0 & 0 < x < 1, \\ u(0,t) = u(1,t) = 1 & 0 < t < t_0, \end{cases} \tag{5.2}$$

where t_0 is the nondimensional reference time. To solve this problem using separation of variables we first need to homogenize the boundary conditions, Therefore consider $w(x,t) = u(x,t) - 1$, which satisfies

$$\begin{cases} w_t - w_{xx} = 0 & 0 < x < 1, \ 0 < t < t_0, \\ w(x,0) = -1 & 0 < x < 1, \\ w(0,t) = w(1,t) = 0 & 0 < t < t_0. \end{cases} \tag{5.3}$$

The solution to (5.3) is

$$w(x,t) = \sum_{n=1}^{\infty} a_n \sin(n\pi x) e^{-(n\pi)^2 t}, \tag{5.4}$$

where

$$a_n = -2 \int_0^1 \sin(n\pi x) dx \tag{5.5}$$

are the Fourier coefficients subject to the initial condition $w(x,0)$. A quick computation shows that

$$a_n = \begin{cases} -\dfrac{4}{\pi n} & \text{if } n \text{ odd}, \\ 0 & \text{if } n \text{ even}. \end{cases} \tag{5.6}$$

Therefore, the solution for small times, i.e., $t < t_0'$, in this first model is

$$u(x,t) = 1 - \sum_{n \ odd} \frac{4}{\pi n} \sin(n\pi x) e^{-(n\pi)^2 t}. \tag{5.7}$$

As shown in figure 5.2, the solution behaves like one would expect, at least in the interior of the film. However, it turns out that this model is not physically realistic, since the laser beam does not set the boundary to a constant temperature, but in reality it can be interpreted as a constant heat flux q_0 through it.

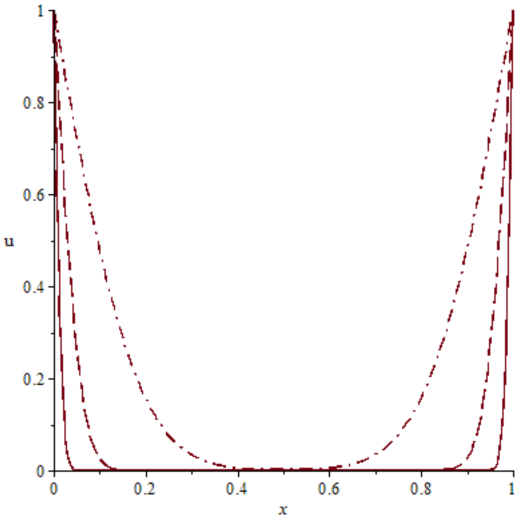

Figure 5.2: Nondimensional solution for $t = 10^{-4}$ (solid line), $t = 10^{-3}$ (dashed line), $t = 10^{-2}$ (dashed-dotted line) using the model with Dirichlet boundary conditions.

5.2 Model with Neumann boundary conditions

Consider now the following model:

$$\begin{cases} T_t - \alpha T_{xx} = 0 & 0 < x < L,\ t > 0, \\ T(x,0) = T_0 & 0 < x < L, \\ kT_x(0,t) = -kT_x(L,t) = q_0 & t < t_0, \\ T_x(0,t) = T_x(L,t) = 0 & t > t_0, \end{cases} \tag{5.8}$$

where q_0 is the heat flux due to the laser. We will again only focus on the case $t < t_0$. We choose $\gamma_x = L$, $\gamma_t = L^2/\alpha$ and $\gamma_T = k/(q_0 L)$ in (2.10) to obtain, after dropping the primes,

$$\begin{cases} u_t - u_{xx} = 0 & 0 < x < 1,\ t < t_0, \\ u(x,0) = 0 & 0 < x < 1, \\ u_x(0,t) = -u_x(1,t) = 1 & t < t_0, \end{cases} \tag{5.9}$$

Define now $w(x,t) = u(x,t) - x(x-1)$, then w satisfies the system

$$\begin{cases} w_t - w_{xx} = 2 & 0 < x < 1,\ t < t_0, \\ w(x,0) = -x(x-1) & 0 < x < 1, \\ w_x(0,t) = w_x(1,t) = 0 & t < t_0. \end{cases} \tag{5.10}$$

Since (5.10) is nonhomogeneous, we can solve the problem by using an eigenfunction expansion. Assume that w is of the form

$$w(x,t) = \frac{a_0(t)}{2} + \sum_{n=1}^{\infty} a_n(t)\cos(n\pi x), \tag{5.11}$$

which satisfies the boundary conditions of (5.10). To compute the unknown terms $a_n(t)$, let us substitute this expression into the equation, which then yields the following system of ordinary differential equations:

$$\begin{aligned} &a_0' = 4, \\ &a_n' + (\pi n)^2 a_n = 0 \quad \text{for } n \geq 1. \end{aligned} \tag{5.12}$$

The initial condition must still hold, and hence let us expand $w(x,0)$ into its expansion with cosine functions to be able to compare it to the expression in (5.11). Notice that $w(x,0)$ does not belong to the space $\{u \in L^2 | u_x(0) = u_x(1) = 0\}$, and hence we have to consider its orthogonal projection $w_p(x)$ into this space

$$w_p(x) = \frac{b_0}{2} + \sum_{n=1}^{\infty} b_n \cos(n\pi x), \tag{5.13}$$

where

$$\begin{aligned} b_0 &= -2\int_0^1 x(x-1)dx = \tfrac{1}{3}, \\ b_n &= -2\int_0^1 x(x-1)\cos(n\pi x)dx. \end{aligned} \tag{5.14}$$

Evaluating b_n yields

$$b_n = \begin{cases} \frac{-4}{n^2\pi^2} & \text{if } n \text{ even} \\ 0 & \text{if } n \text{ odd}, \end{cases} \tag{5.15}$$

The condition $w(x,0) = -x(x-1)$ then is translated into $a_n(0) = b_n$, and therefore, combining with (5.12), it turns out that we have to solve

$$\begin{cases} a_0' = 4 \\ a_0(0) = \frac{1}{3}, \end{cases} \tag{5.16}$$

$$\begin{cases} a_{2k}' + (2k)^2\pi^2 a_{2k} = 0 \\ a_{2k}(0) = \frac{-4}{n^2\pi^2}, \end{cases} \tag{5.17}$$

$$\begin{cases} a_{2k+1}' + (2k+1)^2\pi^2 a_{2k+1} = 0 \\ a_{2k+1}(0) = 0. \end{cases} \tag{5.18}$$

The solutions to these systems are

$$\begin{aligned} &a_0(t) = 4t + \tfrac{1}{3}, \\ &a_{2k}(t) = \tfrac{-4}{(2k)^2\pi^2} e^{-(2k)^2\pi^2 t}, \\ &a_{2k+1}(t) = 0, \end{aligned} \tag{5.19}$$

and hence the solution to (5.10) is

$$w(x,t) = 2t + \frac{1}{6} - \sum_{k=1}^{\infty} \frac{1}{k^2\pi^2} e^{-4k^2\pi^2 t} \cos(2k\pi x). \tag{5.20}$$

Consequently, the solution to (5.9) is given, using (5.13)-(5.15), by

$$u(x,t) = 2t + \sum_{k=1}^{\infty} \frac{1}{k^2\pi^2} \left(1 - e^{-4k^2\pi^2 t}\right) \cos(2k\pi x), \tag{5.21}$$

Figure 5.3 displays the temperature profiles for some values of t. The behaviour is now, at first sight, more realistic than the solution of the first approach, since the temperature of the boundaries of the film becomes higher after being in contact with the laser beam for more time, and the center of the film again takes longer to increase its temperature. However, there are some other concepts that have not been taken into account in this model. For instance, the way the laser propagates through the medium should be taken under consideration.

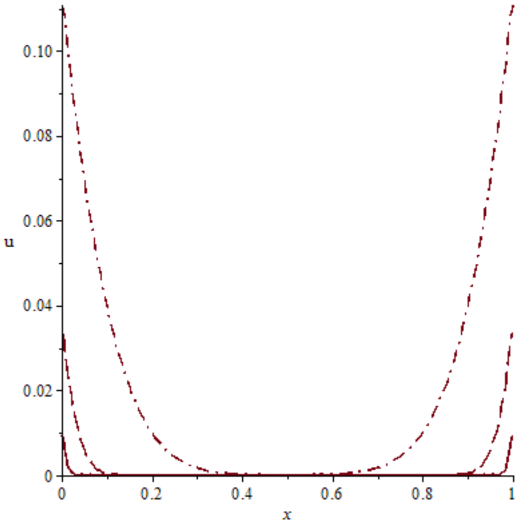

Figure 5.3: Nondimensional solution for $t = 10^{-4}$ (solid line), $t = 10^{-3}$ (dashed line) and $t = 10^{-2}$ (dashed-dotted line) using the model with Neumann boundary conditions.

5.3 Model with an internal heat source

Since the heat of the laser beam penetrates the medium, it does not only affect the boundary and hence a more accurate model which takes this heat penetration into account, is needed. Therefore, suppose the film is insulated and assume that the effect of the laser beam acts as an internal source $g(x,t)$ in the film. Researchers like Torii *et al.* [19] or Lewandowska *et al.* [20] describe this internal heat source as

$$g(x,t) = I(t)(1-R)\mu\left(e^{-\mu x} + e^{-\mu(L-x)}\right), \tag{5.22}$$

where

1) $I(t)$ is the laser incident intensity,

2) R is the surface reflectance of the body,

3) μ is the absorption rate of the body.

The assumption of taking vanishing Neumann boundary conditions might sound arbitrary. It has been reported [21] that almost all the energy is absorbed within a depth of $10^{-7}\mu m$, whence the temperature can be assumed to be constant in a thin layer next to the boundaries of the film.

Since in our situation we are heating the film on both sides until $t = t_0$, I takes the form

$$I(t) = (H(t) - H(t-t_0))\, I_0, \tag{5.23}$$

where $I_0 \gg 0$ and H is the heaviside step function. Let $S(x)$ be the time-independent part of the heat source, then the equations for this model read

$$\begin{cases} T_t - \alpha T_{xx} = (H(t) - H(t-t_0)) \frac{I_0}{c_p \rho} S(x) & 0 < x < L,\ t > 0 \\ T(x,0) = T_0 & 0 < x < L, \\ T_x(0,t) = T_x(L,t) = 0 & t > 0. \end{cases} \tag{5.24}$$

Let us define the nondimensional variables (2.10) by taking again the typical length and time scales $\gamma_x = L$ and $\gamma_t = L^2/\alpha$. The value for γ_T is to be determined. After dropping the primes, the system for u is

$$\begin{cases} u_t - u_{xx} = (H(t) - H(t-t_0)) \frac{I_0 L}{k \gamma_T} (1-R) \eta \left(e^{-\eta x} + e^{-\eta(1-x)}\right) & 0 < x < 1,\ t > 0, \\ u(x,0) = 0 & 0 < x < 1, \\ u_x(0,t) = u_x(1,t) = 0 & t > 0, \end{cases} \tag{5.25}$$

where $\eta = L\mu$. Choosing $\gamma_T = I_0 L(1-R)/k$ simplifies the equation and ensures the laser heating as the dominant driving force.

We solve this problem using Duhamel's method for the classical heat equation [1]. First, let f be the nondimensional heat source, i.e.,

$$f(x,t) = (H(t) - H(t-t_0))\, \eta \left(e^{-\eta x} + e^{-\eta(1-x)}\right), \tag{5.26}$$

and let $u(x,t;s)$ be the solution to

$$\begin{cases} u_t(x,t;s) - u_{xx}(x,t;s) = 0, & 0 \le x \le 1, t > s, \\ u_x(0,t;s) = u_x(1,t;s) = 0, & t \ge 0, \\ u(x,s;s) = f(x,s), & 0 \le x \le 1, \end{cases} \tag{5.27}$$

The solution to (5.25) is then given by

$$u(x,t) = \int_0^t u(x,t;s) ds. \tag{5.28}$$

Let us show that u solves (5.25). Its derivatives are

$$\begin{aligned} &u_t(x,t) = u(x,t;t) + \textstyle\int_0^t u_t(x,t;s) ds = f(x,t) + \int_0^t u_t(x,t;s) ds, \\ &u_{xx}(x,t) = \textstyle\int_0^t u_{xx}(x,t;s) ds, \end{aligned} \tag{5.29}$$

hence u satisfies the equation $u_t - u_{xx} = f$. The boundary and initial conditions are trivially satisfied due to the definition of u.

The solution to (5.27) can be computed in an analogous way as in (5.10). Since the boundary conditions are of Neumann type, consider the expansion of $u(x,t;s)$ as follows,

$$u(x,t;s) = \frac{a_0(t)}{2} + \sum_{n=1}^{\infty} a_n(t) \cos(n\pi x), \tag{5.30}$$

which clearly satisfies the homogeneous boundary conditions of the problem. Since one has that

$$u(x,s;s) = f(x,s), \tag{5.31}$$

let us give the expansion of f in order to compare both sides of (5.31). This expansion is

$$f(x,s) = (H(s) - H(s-t_0))\left(\frac{b_0}{2} + \sum_{n=1}^{\infty} b_n \cos(n\pi x)\right), \tag{5.32}$$

where

$$b_n = 2\int_0^1 f(x)\cos(n\pi x)dx,\ n \geq 0 \tag{5.33}$$

A quick computation yields

$$\begin{array}{ll} b_0 = 4\left(1-e^{-\eta}\right), & \\ b_{2k} = \frac{4\eta\left(1-e^{-\eta}\right)}{\eta^2+(2k)^2\pi^2}, & k>0 \\ b_{2k+1} = 0, & k \geq 0, \end{array} \tag{5.34}$$

Combining (5.30)-(5.32), we obtain

$$a_n(s) = (H(s) - H(s-t_0))\, b_n, \tag{5.35}$$

and substituting (5.30) into (5.27) we obtain the following system of ODE's

$$\left\{ \begin{array}{l} a_0' = 0 \\ a_0(s) = 4\left(1-e^{-\eta}\right)(H(s) - H(s-t_0)), \end{array}\right. \tag{5.36}$$

$$\left\{ \begin{array}{l} a_{2k}' + (2k)^2\pi^2 a_{2k} = 0 \\ a_{2k}(s) = \frac{4\eta\left(1-e^{-\eta}\right)}{\eta^2+(2k)^2\pi^2}(H(s) - H(s-t_0)), \end{array}\right. \tag{5.37}$$

$$\left\{ \begin{array}{l} a_{2k+1}' + (2k+1)^2\pi^2 a_{2k+1} = 0 \\ a_{2k+1}(s) = 0, \end{array}\right. \tag{5.38}$$

whose solutions are given by

$$a_0(t;s) = 4\left(1-e^{-\eta}\right)(H(s) - H(s-t_0)), \tag{5.39}$$

$$a_{2k}(t;s) = \frac{4\eta\left(1-e^{-\eta}\right)}{\eta^2+(2k)^2\pi^2} e^{-(2k\pi)^2(t-s)}(H(s) - H(s-t_0)), \tag{5.40}$$

$$a_{2k+1}(t;s) = 0. \tag{5.41}$$

Therefore, the solution to the auxiliary system (5.27) is given by

$$u(x,t;s) = 4\left(1-e^{-\eta}\right)\left[\frac{1}{2} + \sum_{k=1}^{\infty} \frac{1}{\eta^2+(2k\pi)^2} e^{-(2k\pi)^2(t-s)}\cos(2k\pi x)\right](H(s) - H(s-t_0)), \tag{5.42}$$

and, using (5.28), we have that the solution to (5.25) is

$$u(x,t) = \left\{ \begin{array}{ll} 4\left(1-e^{-\eta}\right)\left[\frac{t}{2} + \sum_{k=1}^{\infty} \frac{1-e^{-(2k)^2\pi^2 t}}{(2k)^2\pi^2(\eta^2+(2k)^2\pi^2)}\cos(2k\pi x)\right] & t<t_0, \\ 4\left(1-e^{-\eta}\right)\left[\frac{t_0}{2} + \sum_{k=1}^{\infty} \frac{e^{-(2k)^2\pi^2(t-t_0)} - e^{-(2k)^2\pi^2 t}}{(2k)^2\pi^2(\eta^2+(2k)^2\pi^2)}\cos(2k\pi x)\right] & t>t_0. \end{array}\right. \tag{5.43}$$

Considering a slab of thickness $L = 0.01m$ does not yield realistic results as it can be observed in figure 5.5, where we see that the temperature is almost constant along

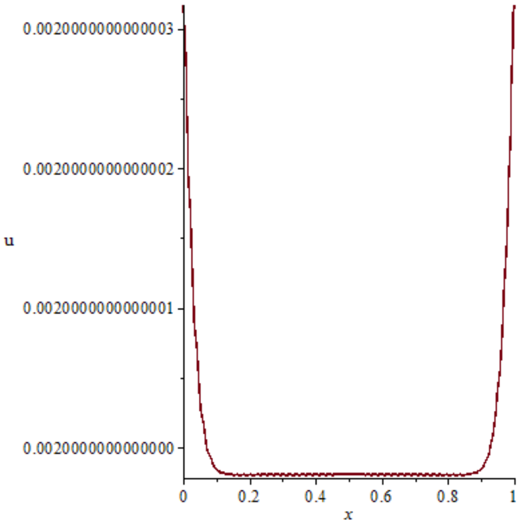

Figure 5.4: Nondimensional temperature profile for $t = 0.001$. The value for η has been assumed to be of the order of 10^5, corresponding to a thickness of $L = 0.01m$ and an absorbtion rate of $\mu = 10^7 m^{-1}$, which is a typical value for most metals [19].

the whole slab in every time step. In fact, the term $\eta^2 \sim 10^{10}$ in the denominator of the terms in the series reduces u basically to a linear function of time, since the terms in the series are, at least, of order 10^{-10}. Nevertheless, the effect of the heat source can be observed in figure 5.4, although the differences in the temperature at the boundaries and at the center of the slab is almost negligible. This model therefore fails if one considers a relatively thick slab or a medium with a high absorption rate.

On the other hand, figure 5.6 shows that the temperature becomes constant quickly right after the heat source disappears. This is a direct consequence of assuming the walls of the slab to be insulated. Therefore this model just has sense until few seconds after removing the heat sources, since the film in the end will adapt its temperature to the values of its environment.

For a thickness of the order of $10^{-6}m$ figure 5.7 shows a physically more realistic behaviour. The temperature increases in time, but the boundary is always hotter than the center of the slab. However, the linear term in (5.43) still retains the idea of infinite speed of propagation, which can be avoided using Cattaneo's model.

5.4 Model using the Maxwell-Cattaneo equations

Consider the same boundary conditions as in the previous attempt, but let us now assume that the governing equation is given by the Maxwell-Cattaneo model, i.e.

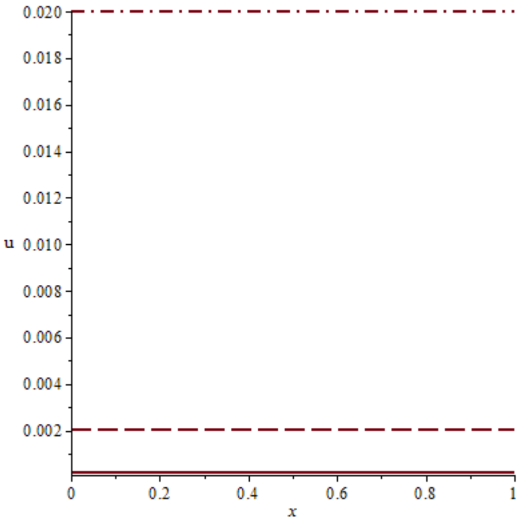

Figure 5.5: Nondimesional temperature profiles for $t = 10^{-4}$ (solid line), $t = 10^{-3}$ (dashed line) and $t = 10^{-2}$ (dashed-dotted line).

consider

$$\begin{cases} \tau_0 T_{tt} + T_t - \alpha T_{xx} = \dfrac{I_0}{c_p \rho} S(x) R(t) & 0 < x < L,\ t > 0, \\ T(x, 0) = T_0 & 0 < x < L, \\ T_t(x, 0) = 0 & 0 < x < L, \\ T_x(0, t) = T_x(L, t) = 0 & t > 0, \end{cases} \tag{5.44}$$

where $R(t) = H(t) - H(t - t_0) + \tau_0 \delta_0(t) - \tau_0 \delta_0(t - t_0)$. Applying the same nondimensional variables as in the previous model the equations are

$$\begin{cases} \epsilon_0 u_{tt} + u_t - u_{xx} = \eta \left(e^{-\eta x} + e^{-\eta(1-x)} \right) R(t) & 0 < x < 1,\ t > 0 \\ u(x, 0) = 0 & 0 < x < 1, \\ u_t(x, 0) = 0 & 0 < x < 1, \\ u_x(0, t) = u_x(1, t) = 0 & t > 0. \end{cases} \tag{5.45}$$

As before, $f(x, t)$ is the nondimensional heat source. Let us recall the Solution Structure Theorem, that states that the solution to (5.45) is of the form

$$u(x, t) = \int_0^t w(x, t; s) ds, \tag{5.46}$$

where w solves

$$\begin{cases} \epsilon_0 w_{tt} + w_t - w_{xx} = 0 & 0 < x < 1,\ t > s \\ w(x, s; s) = 0 & 0 < x < 1, \\ w_t(x, s; s) = f(x, s) & 0 < x < 1, \\ w_x(0, t; s) = w_x(1, t; s) = 0 & t > s. \end{cases} \tag{5.47}$$

Using Duhamel's method introduced in chapter 3 we obtain

$$w(x, t; s) = \frac{T_0(t; s)}{2} + \sum_{n=1}^{\infty} T_n(t; s) \cos(n \pi x), \tag{5.48}$$

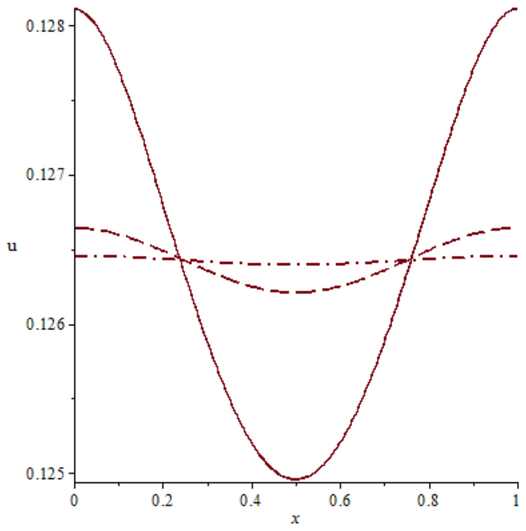

Figure 5.6: Nondimensional temperature profiles for $t = 0.1$ (solid line), $t = 0.15$ (dashed line) and $t = 0.2$ (dashed-dotted line) after heating the slab until $t_0 = 0.1$.

where T_n are the solutions to

$$\begin{aligned} &\epsilon_0 T_0'' + T_0' = 0, \\ &\epsilon_0 T_n'' + T_n' + (n\pi)^2 T_n = 0, \quad n > 0. \end{aligned} \tag{5.49}$$

Using $w(x, s; s) = 0$ we obtain

$$T_n(s) = 0, \tag{5.50}$$

and $w_t(x, s; s) = f(x, s)$ yields

$$T_n'(s) = b_n R(s), \tag{5.51}$$

where the coefficients b_n are defined in (5.34). The expression of T_0 is

$$T_0(t; s) = \epsilon_0 b_0 \left(1 - e^{-(t-s)/\epsilon_0}\right) R(s), \tag{5.52}$$

whilst the expression of T_n for $n > 0$ has already been derived in (3.44), although a translation in time is needed in this case. All in all, the expression of T_n is

$$T_n(t; s) = \begin{cases} A_n(s) e^{\frac{\sqrt{\Delta_n}-1}{2\epsilon}(t-s)} + B_n(s) e^{-\frac{\sqrt{\Delta_n}+1}{2\epsilon}(t-s)} & \text{if } n < n_0, \\ e^{-\frac{(t-s)}{2\epsilon}} \left[C_n(s) \sin\left(\frac{\sqrt{-\Delta_n}}{2\epsilon}(t-s)\right) + D_n(s) \cos\left(\frac{\sqrt{-\Delta_n}}{2\epsilon}(t-s)\right)\right] & \text{if } n > n_0. \end{cases} \tag{5.53}$$

where the unknown coefficients are defined in (3.48). Using the initial conditions (5.50) and (5.51) we finally obtain

$$\begin{aligned} A_n(s) &= \tfrac{\epsilon_0 b_n}{\sqrt{\Delta_n}} R(s), \\ B_n(s) &= -\tfrac{\epsilon_0 b_n}{\sqrt{\Delta_n}} R(s), \\ C_n(s) &= \tfrac{2\epsilon_0 b_n}{\sqrt{-\Delta_n}} R(s), \\ D_n(s) &= 0, \end{aligned} \tag{5.54}$$

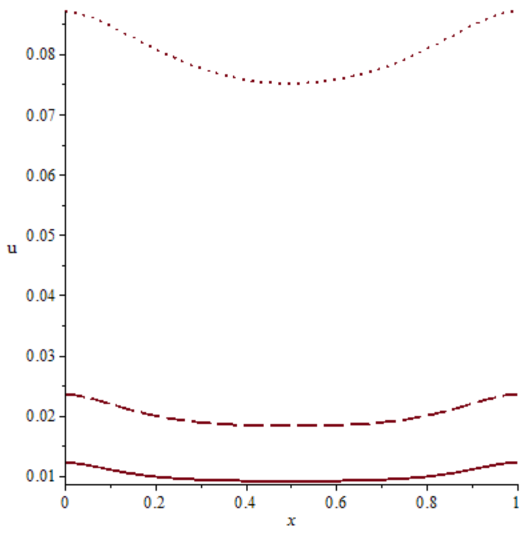

Figure 5.7: Nondimensional temperature profile for $t = 0.005$ (solid line), $t = 0.01$ (dashed line), $t = 0.04$ (dotted line) when considering a thickness $L = 10^{-6}m$.

which yields

$$T_n(t;s) = \begin{cases} \frac{2\epsilon_0 b_n}{\sqrt{\Delta_n}} e^{-(t-s)/2\epsilon_0} \sinh\left(\frac{\sqrt{\Delta_n}}{2\epsilon}(t-s)\right) R(s) & \text{if } n < n_0, \\ \frac{2\epsilon_0 b_n}{\sqrt{-\Delta_n}} e^{-(t-s)/2\epsilon_0} \sin\left(\frac{\sqrt{-\Delta_n}}{2\epsilon}(t-s)\right) R(s) & \text{if } n > n_0. \end{cases} \tag{5.55}$$

The solution to (5.45) is therefore

$$u(x,t) = \frac{1}{2}\int_0^t T_0(t;s)ds + \sum_{n=1}^{\infty} \int_0^t T_n(t;s)ds \cos(n\pi x). \tag{5.56}$$

The integrales involved in (5.56) can be computed explicitely. Let $C_n(t;s)$ be the factor of $T_n(t;s)$ that multiplies $R(s)$, i.e., $T_n(t;s) = C_n(t;s)R(s)$. Thus,

$$\begin{aligned} \textstyle\int_0^t T_n(t;s)ds &= \textstyle\int_0^t C_n(t;s)R(s)ds \\ &= \textstyle\int_0^t C_n(t;s)(H(s) - H(s-t_0))ds + \tau_0 \int_0^t C_n(t;s)\delta_0(s)ds \\ &\quad -\tau_0 \textstyle\int_0^t C_n(t;s)\delta_0(s-t_0)ds \\ &= (1)\ +\ (2)\ +\ (3). \end{aligned} \tag{5.57}$$

Let us compute each term separately.

$$\begin{aligned} (1) &= \textstyle\int_0^t C_n(t;s)\left((H(s) - H(s-t_0)\right)ds \\ &= \textstyle\int_0^{\min(t,t_0)} C_n(t;s)ds \end{aligned} \tag{5.58}$$

These integrals can be computed explicitely,

$$(1) = \begin{cases} \epsilon_0 b_0 \left(s - \epsilon_0 e^{-(t-s)/\epsilon_0}\right)\Big|_{s=0}^{s=\min(t,t_0)} & n = 0, \\ \frac{2b_n\epsilon_0^2 e^{-(t-s)/(2\epsilon_0)}}{\sqrt{\Delta_n}(\Delta_n - 1)} \left(\sqrt{\Delta_n}\cosh\left(\frac{\sqrt{\Delta_n}}{2\epsilon_0}(t-s)\right) - \sinh\left(\frac{\sqrt{\Delta_n}}{2\epsilon_0}(t-s)\right)\right)\Big|_{s=0}^{s=\min(t,t_0)} & 0 < n < n_0, \\ \frac{2b_n\epsilon_0^2 e^{-(t-s)/(2\epsilon_0)}}{\sqrt{-\Delta_n}(1 - \Delta_n)} \left(\sqrt{-\Delta_n}\cos\left(\frac{\sqrt{-\Delta_n}}{2\epsilon_0}(t-s)\right) - \sin\left(\frac{\sqrt{-\Delta_n}}{2\epsilon_0}(t-s)\right)\right)\Big|_{s=0}^{s=\min(t,t_0)} & n > n_0. \end{cases} \tag{5.59}$$

On the other hand,

$$\begin{aligned}(2) \quad &= \tau_0 \int_0^t C_n(t;s)\delta_0(s)ds \\ &= \tau_0 C_n(t;0),\end{aligned} \tag{5.60}$$

and

$$\begin{aligned}(3) \quad &= \tau_0 \int_0^t C_n(t;s)\delta_0(s-t_0)ds \\ &= \begin{cases} 0 & \text{if } t < t_0, \\ \tau_0 C_n(t;t_0) & \text{if } t \geq t_0, \end{cases}\end{aligned} \tag{5.61}$$

therefore we have finally found the explicit expression for (5.56).

Lewandowska *et al.* [20] provided an analytical solution to this model via Laplace transforms, while Torii *et al.* [19] used the method of finite differences to obtain an approximate solution. Here we have used the technique of eigenfunction expansion and the Solution Structure Theorem to solve the problem.

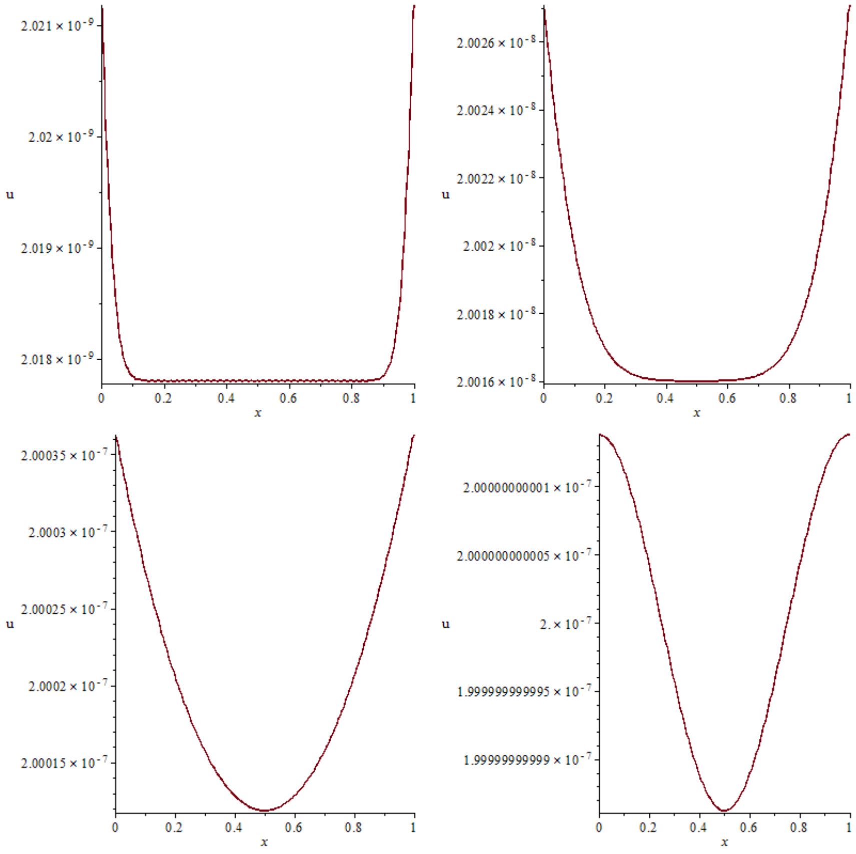

Figure 5.8: Time evolution of the nondimensional temperature for $t \in (0.01, 0.5)$. The values of the parameters are $\alpha = 10^{-7} m^2/s$, $\mu = 10^7 m^{-1}$, $L = 10^{-3} m$, $t_0 = 10^{-6} s$, $\tau_0 = 10^{-5} s$.

In figure 5.8 we see that the solution displays a diffusive behaviour for relatively large values of L. The differences in temperature along the slab are minimal in each time step. This is due to the large value of η, which minimizes the impact of the terms in the series (5.56).

Assume now $L = 10^{-6}m$. In figure 5.9 we can clearly observe two waves starting each one in one extreme of the slab, and travelling inside it in opposite directions until they collide in the center of the film at $t = 0.5$ and again at $t = 1.5$, which in dimensional variables means that the speed of propagation of the thermal wave is $c = 10^{-1}m/s$. This is exactly the value determined by the relation $c^2 = \alpha/\tau_0$. However, this behaviour disappears as t_0 increases, as it can be seen in figure 5.10, where the temperature gradually increases along the whole film as the time increases. These results are qualitatively in good agreement with the results provided in [19, 20].

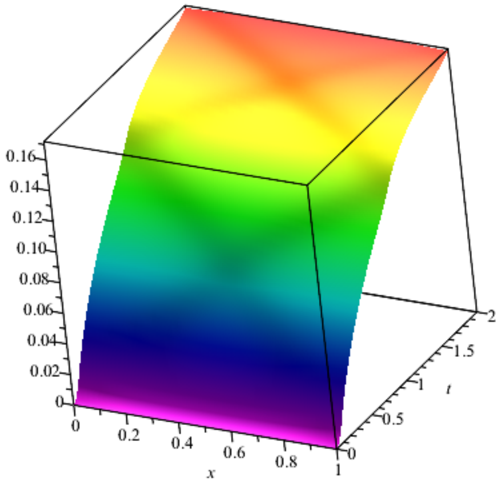

Figure 5.9: 3-dimensional plot of the solution when $L = 10^{-6}m$ and hence $\epsilon_0 = 1$ and $\eta = 10$. The slab is heated until $t_0 = 10^{-6}s$.

5.5 Results

In the first model we observe that the temperature of the walls is constant for $t > 0$, which cannot be possible since the heat of the laser beam is suposed to increase it. This problem is solved in the second model, where the laser beam is modeled as a constant heat flux across the walls. Although the results seem to be credible, properties of the medium such as surface reflectance or thermal absorption are neglected and hence the model is not physically consistent. These properties are taken into account in the last two models, where the laser beam is modeled as a inner heat source and the slab is assumed to be insulated. This can be argued by saying that the effect of the laser is quickly and almost entirely absorbed in a thin layer next to the boundary, and hence the instantanteous temperature in these layers is constant. Due to the high absorption coefficient, the third model, where the governing heat equation has been assumed to be the classical one, fails for thick films because during the heating process the solution behaves as a linear function of time, constant along the whole film. This behaviour is weaker as the thickness of the film decreases, but a term linear in time and constant in space is still preserving the idea of infinite speed of propagation. This speed of propagation is finite in the last model, where the governing equation of heat

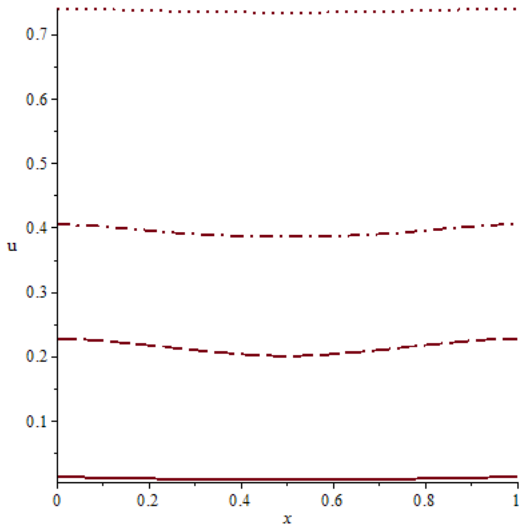

Figure 5.10: Evolution of the nondimensional temperature of the slab with $L = 10^{-6}m$ until $t_0 = 10^{-5}s$.

is the hyperbolic heat equation. We can clearly observe two waves approaching each other with the thermal speed provided by the model, and colliding in the center of the film, where a temperature overshoot takes place. When reaching the opposite wall of the film, the heat waves turn around and travel again through the slab. The amplitude of these waves decreases in time until they disappear and the temperature in the film becomes constant. On the other hand, when considering thicker materials we see that the wavelike behaviour tends to disappear and we recover again a diffusive character.

This last model clearly shows two behaviours of the solutions depending on the heating time t_0 and the thickness L of the film, which is expected to happen as it has been reported [19, 20, 21], and hence seems to be the most reliable of the four theoretical models that have been discussed.

6

Heating of Biological Tissue

6.1 Thermal models for biological tissue. Pennes bioheat equation

Modern surgery has developed several techniques based on the punctual heating of biological tissues, either extracting (cryosurgery) [25] or intruducing heat (laser, microwave, radiofrequency current)[28, 29]. Since they are not as intrusive as other traditional techniques, they establish a new and, in principle, safer field of medical treatments.

Pennes considered Fourier's theory of heat conduction in order to introduce the *bioheat equation* [24]

$$\rho c_p T_t = \nabla \cdot (k \nabla T) + S_m + S_p, \tag{6.1}$$

which is equivalent to (2.2), where the heat source S has been split into two groups:

1) S_m refers to the metabolic activity of the biological system,
2) S_p denotes the heat that arises through blood perfusion, i.e., the temperature difference between the blood entering and exiting the tissue.

Since this equation corresponds exactly to the parabolic equation introduced in chapter 2, we will avoid the theoretical study on this equation. However, we will use the solutions to this equation to compare them with the hyperbolic model.

Methods like laser thermokeratoplasty (LTK) or radiofrequency heating (RFH) involve very small time scales and high energy fluxes, and therefore the parabolic model may not be appropiate. The way to argue this is that thermal equilibrium cannot be reached on small time scales $t \in [0, \tau_0]$, according to our definition of τ_0 given in chapter 3. Therefore we will employ the hyperbolic model to establish a theoretically more appropiate description of these processes. The equation we want to solve is given by

$$\tau_0 T_{tt} + T_t - \alpha \Delta T = \frac{1}{\rho c_p} \left(S + \tau_0 S_t \right), \tag{6.2}$$

where $S = S_m + S_p + S_s$. The new source term S_s refers to the surgical heat source.

6.2 Mathematical study of RFH

RFH is employed in several clinical areas such as destruction of tumors and heating of the cornea for refroactive surgery, for instance [33]. We will focus now on this last example, also called conductive keratoplasty (CK).

This technique is used to reduce visual problems such as myopia, for instance, and a part of the procedure consists in inserting a small electrode into the cornea in order to deliver a small amount of energy (less than $0.6W$), to the corneal stroma for a short period of time, not longer than $600ms$. The temperature of the cornea therefore increases, but it cannot exceed 70^oC since that would cause serious damage and even the total loss of sight.

Therefore, a mathematical model is needed in order to predict the evolution of the temperature of the cornea in order to improve the technique and obtain better and more accurate results. The classical model in order to describe the evolution of the temeprature profile relies on Fourier's model of the heat conduction, but in our case we are going to study the model using the model by Cattaneo.

In our model we consider a spherical electrode of radius r_0 which is in close contact with the cornea. We assume $S_p = S_m = 0$, which is admissible for the cornea since it is a non-perfused tissue. The cornea is assumed to have infinite dimensions, since it is much larger than the inserted electrode. Therefore the problem displays radial symmetry and hence the spatial variables can be reduced to the radial variable. The source term $S = S_s$ is modeled as a product of a temporal and a radial part

$$S(r,t) = S(r)H(t) = \frac{Pr_0}{4\pi r^4}H(t). \tag{6.3}$$

The radial part S is due to Erez and Shitzer [32], and P is the total applied power (W).

The temporal part is the Heaviside function, and it indicates that we are considering a non-pulsed source. For a pulsed source the temporal term would be $H(t)-H(t-t_0)$, where t_0 would be the period of action of the electrode. The equation to solve is

$$\tau_0 T_{tt} + T_t - \frac{\alpha}{r^2}\partial_r\left(r^2 T_r\right) = \frac{Pr_0}{4\pi r^4 \rho c_p}\left(H + \tau_0\delta_0\right). \tag{6.4}$$

Notice that we have relaxed the definition of derivative to a weaker sense [1] in order to be able to differentiate H. The initial conditions for (6.4) are

$$\begin{aligned} T(r,0) &= T_0, \\ T_t(r,0) &= 0, \end{aligned} \tag{6.5}$$

and we now derive the boundary conditions for the model. The first condition that has to be considered is

$$\lim_{r\to\infty} T(r,t) = T_0,\ \forall t > 0, \tag{6.6}$$

because we consider that the effect of the electrode does not reach the limit of the cornea since it acts only for a very short period of time and the dimensions of the cornea are much larger than the electrode itself.

To find the boundary condition on $r = r_0$ we have to include a simplification in the model. We assume that the conductivity of the electrode is much higher than that of the cornea, which means that the boundary condition at the interface depends mainly on the thermal inertia of the electrode. The boundary condition then arises from the condition

$$\int_{r=r_1} \mathbf{q}(r,t) \cdot \mathbf{n} d\sigma = \int_{r \leq r_1} \rho_0 c_0 T_t(r,t) dV, \tag{6.7}$$

for all $r_1 \leq r_0$, i.e., that the rate of change of the total temperature in a spherical volume contained in the electrode is equal to the amount of heat crossing its surface. The quantities ρ_0 and c_0 are the density and the specific heat of the electrode. Using (3.23) and setting $r_1 = r_0$ we obtain

$$\int_{r=r_0} \left(\frac{k}{\tau_0} \int_0^t e^{s/\tau_0} \nabla T(r,s) ds \right) \cdot \mathbf{n} d\sigma = \rho_0 c_0 \frac{4\pi r_0^3}{3} T_t(r_0,t) e^{t/\tau_0}. \tag{6.8}$$

In order to obtain the this equation, we have assumed that the electrode's thermal conductivity to be relatively high and its r_0 relatively small, so that the electrode acts as a punctual heat source, which justifies taking T_t outside the integral. Now, since $\nabla T \cdot \mathbf{n} = T_r$ in a spherical surface, we finally obtain

$$4\pi r_0^2 \frac{k}{\tau_0} \int_0^t e^{s/\tau_0} T_r(r_0,t) ds = \rho_0 c_0 \frac{4\pi r_0^3}{3} T_t(r_0,t) e^{t/\tau_0}, \tag{6.9}$$

and, differentiating with respect to t, the condition finally reads

$$\tau_0 T_{tt}(r_0,t) + T_t(r_0,t) = \frac{3k}{\rho_0 c_0 r_0} T_r(r_0,t), \ \forall t > 0. \tag{6.10}$$

Thus, the entire problem reads

$$\begin{cases} \tau_0 T_{tt} + T_t - \dfrac{\alpha}{r^2} \partial_r \left(r^2 T_r \right) = \dfrac{P r_0}{4\pi r^4 \rho c_p} \left(H + \tau_0 \delta_0 \right) & \\ T(r,0) = T_0, & \forall r > r_0, \\ T_t(r,0) = 0, & \forall r > r_0, \\ \lim\limits_{r \to \infty} T(r,t) = T_0, & \forall t > 0, \\ \tau_0 T_{tt}(r_0,t) + T_t(r_0,t) = \dfrac{3k}{\rho_0 c_0 r_0} T_r(r_0,t), & \forall t > 0. \end{cases} \tag{6.11}$$

To find an analytical solution to the problem we will use the following nondimensional quantities

$$\begin{aligned} r' = \frac{r}{r_0}, \ t' = \frac{\alpha t}{r_0^2}, \\ u' = \frac{4\pi k r_0}{P} T, \ u_0' = \frac{4\pi k r_0}{P} T_0. \end{aligned} \tag{6.12}$$

The nondimensional problem, after dropping the primes, is

$$\begin{cases} \lambda u_{tt} + u_t - u_{rr} - \frac{2}{r} u_r = \dfrac{1}{r^4} \left(H + \lambda \delta_0 \right) & \\ u(r,0) = u_0, & \forall r > 1, \\ u_t(r,0) = 0, & \forall r > 1, \\ \lim\limits_{r \to \infty} u(r,t) = u_0, & \forall t > 0, \\ u_t(1,t) + \lambda u_{tt}(1,t) = \frac{3}{m} u_r(1,t), & \forall t > 0, \end{cases} \tag{6.13}$$

where $m = \dfrac{\rho_0 c_0}{\rho c_p}$ is the dimensionless thermal inertia of the electrode and $\lambda = \alpha\tau_0/r_0^2$ the dimensionless relaxation time. The solution to (6.13) will depend not only on r, t, but also on λ, m. Therefore, we use the notation $u(r, t, \lambda, m)$.

To obtain an homogeneous problem, we will consider the translated function

$$v(r,t) = u(r,t) - u_0 \tag{6.14}$$

and hence the new problem is

$$\begin{cases} \lambda v_{tt} + v_t - v_{rr} - \dfrac{2}{r} v_r = \frac{1}{r^4}\left(H + \lambda\delta_0\right) & \\ v(r,0) = 0, & \forall r > 1, \\ v_t(r,0) = 0, & \forall r > 1, \\ \lim\limits_{r\to\infty} v(r,t) = 0, & \forall t > 0, \\ v_t(1,t) + \lambda v_{tt}(1,t) = \frac{3}{m} v_r(1,t), & \forall t > 0. \end{cases} \tag{6.15}$$

Let us give the ansatz for solving this problem taking Laplace transforms. For the complete solution we refer to [28], since at some point we need to compute an inverse transform, an issue we don't want to focus on. The governing equation in (6.27) becomes

$$(s + \lambda s^2)\tilde{v} - \tilde{v}_{rr} - \frac{2}{r}\tilde{v}_r = \frac{1}{r^4}\left(\frac{1}{s} + \lambda\right). \tag{6.16}$$

where $\tilde{v} = \mathcal{L}_t\{v\}$ and where we have used the formulae [23]

$$\mathcal{L}_t\{H\}(s) = \frac{1}{s},\ \mathcal{L}_t\{\delta_0\}(s) = 1. \tag{6.17}$$

Let us apply a new change of variable by setting

$$w = r\tilde{v}, \tag{6.18}$$

which yields the equation

$$A(s,\lambda)w - w_{rr} = \frac{1}{r^3}\left(\frac{1}{s} + \lambda\right), \tag{6.19}$$

where $A(s,\lambda) = s + \lambda s^2$. Using now the variation of parameters method we obtain

$$\begin{aligned} w(r,s,\lambda,m) = \quad & \left(-\frac{1}{2\sqrt{A(s,\lambda)}}\left(\frac{1}{s}+\lambda\right)\int_1^r \frac{e^{-\sqrt{A(s,\lambda)}u}}{u^3}du + M_1(s,\lambda)\right)e^{\sqrt{A(s,\lambda)}r} \\ & + \left(\frac{1}{2\sqrt{A(s,\lambda)}}\left(\frac{1}{s}+\lambda\right)\int_1^r \frac{e^{\sqrt{A(s,\lambda)}u}}{u^3}du + M_2(s,\lambda)\right)e^{-\sqrt{A(s,\lambda)}r}, \end{aligned} \tag{6.20}$$

and hence

$$\begin{aligned} \tilde{v}(r,s,\lambda,m) = \quad & \frac{1}{r}\left(-\frac{1}{2\sqrt{A(s,\lambda)}}\left(\frac{1}{s}+\lambda\right)\textstyle\int_1^r \dfrac{e^{-\sqrt{A(s,\lambda)}u}}{u^3}du + M_1(s,\lambda)\right)e^{\sqrt{A(s,\lambda)}r} \\ & + \frac{1}{r}\left(\frac{1}{2\sqrt{A(s,\lambda)}}\left(\frac{1}{s}+\lambda\right)\textstyle\int_1^r \dfrac{e^{\sqrt{A(s,\lambda)}u}}{u^3}du + M_2(s,\lambda)\right)e^{-\sqrt{A(s,\lambda)}r}, \end{aligned} \tag{6.21}$$

where the quantities $M_1,\ M_2$ are chosen in order to satisfy the transformed boundary conditions

$$\lim_{r\to\infty} \tilde{v}(r,s,\lambda,m) = 0, \tag{6.22}$$

$$A(s,\lambda)\tilde{v}(1,s,\lambda,m) = \frac{3}{m}\partial_r \tilde{v}(1,s,\lambda,m), \tag{6.23}$$

Condition (6.22) is clearly satisied by taking

$$M_1(s,\lambda) = \frac{1}{2\sqrt{A(s,\lambda)}}\left(\frac{1}{s}+\lambda\right)\int_1^\infty \frac{e^{\sqrt{A(s,\lambda)}u}}{u^3}du, \tag{6.24}$$

since the second term vanishes as $r \to \infty$. Finally, condition (6.23) yields the expression for $M_2(s,\lambda)$ after substituting $\tilde{v}$ in it. We obtain

$$M_2(s,\lambda) = -\frac{e^{2\sqrt{A(s,\lambda)}}}{2\sqrt{A(s,\lambda)}}\left(\frac{1}{s}+\lambda\right)\frac{mA(s,\lambda)-3\sqrt{A(s,\lambda)}+3}{mA(s,\lambda)+3\sqrt{A(s,\lambda)}+3}\int_1^\infty \frac{e^{-\sqrt{A(s,\lambda)}u}}{u^3}du. \tag{6.25}$$

The dimensionless temperature is given by the inverse Laplace transform of (6.21), and thus

$$u(r,t,\lambda,m) = u_0 + \mathcal{L}_s^{-1}\{\tilde{v}\} \tag{6.26}$$

As said before, to complete these computations we refer [28].

Let u^0 be the solution to the limit problem of 6.27 when $\lambda \to 0$, i.e.,

$$\begin{cases} u_t - u_{rr} - \frac{2}{r}u_r = \frac{1}{r^4}H & \\ u(r,0) = u_0, & \forall r > 1, \\ u_t(r,0) = 0, & \forall r > 1, \\ \lim\limits_{r\to\infty} u(r,t) = u_0, & \forall t > 0, \\ u_t(1,t) = \frac{3}{m}v_r(1,t), & \forall t > 0. \end{cases} \tag{6.27}$$

It is possible to compute u^0 with the same methods as u, we refer again to [28] for the details.

6.3 Results

The results are based on the insertion of an active electrode of radius $r_0 = 45\mu m$ into the cornea, which then applies a power of $30mW$ for $600ms$. The applied power has been chosen to mantain the maximal temperature below $120^o C$, and therefore the power level is not comparable to those employed clinically, but it might be important in this study to highlight qualitative differences of the considered models. It has been reported [29] that for materials with a nonhomogeneous inner structure display thermal relaxation time ranging between $10s$ and $50s$. Since the inner structure of the cornea is more homogeneous than the considered materials, the relaxation time of the cornea has been set, as a first approximation, to $\tau_0 = 0.1s$.

As shown in figure 6.1, we observe that for early times the temperature next to the cornea is higher in the HHE model than in the CHE model. This trend becomes negligible as time increases, and finally both temperature profiles become similar at $t = 600ms$, although the HHE solution is always greater than the CHE solution. We observe a cuspidal singularity traveling along the cornea. However, this singularity becomes negligible as time increases. In fact, this singularity travels along the tissue with a speed of $1.25mm/s$, which corresponds to the propagation speed predicted by the formula $c^2 = \alpha/\tau_0$ assuming α to be of the order of $10^{-7}m^2/s$.

In figure 6.2 we observe that in the HHE model the the temperature exceeds very the critical value of 70^oC, whilst the CHE solution never exceeds this value during the whole process.

Differences between the HHE and CHE models are greater at early times and shorter distances, exactly there where the CHE model is not accurate anymore [28, 29, 30, 31]. Therefore, in these cases the HHE model should be considered to avoid, for instance, irreversible damages in the corneal surface.

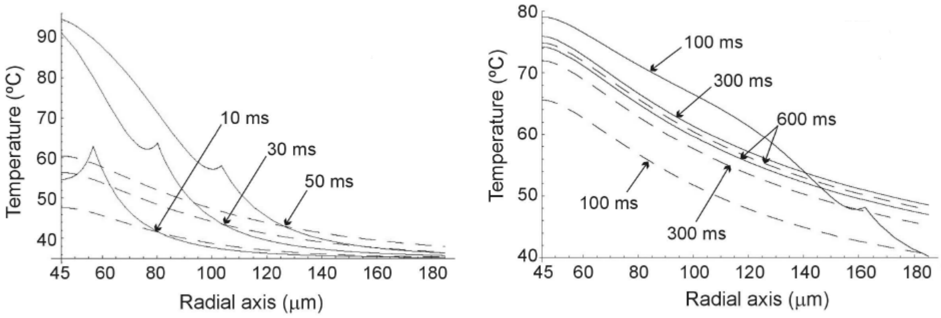

Figure 6.1: Temperature distribution during CK along the radial axis for different times, from $10ms$ to $600ms$, and for the hyperbolic (solid line) and classical (dashed line) heat transfer equations. Considered radius of the electrode $r_0 = 45\mu m$, applied power $P = 30mW$, thermal relaxation time of the cornea $\tau_0 = 100ms$. Plot originally from [29].

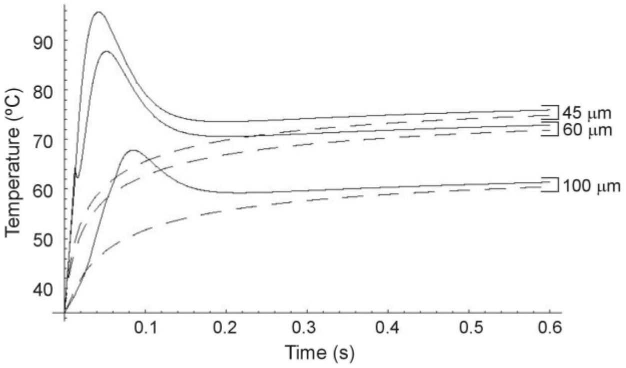

Figure 6.2: Temperature evolution during the CK predicted by the HHE model (solid line) and CHE model (dashed line) at three locations of the cornea: on the electrode surface ($r = 45\mu m$), at $15\mu m$ ($r = 60\mu m$) and at $55\mu m$ ($r = 100\mu m$) from the surface. Applied power $P = 30mW$, thermal relaxation time $\tau_0 = 0.1s$.

7
Conclusions

7.1 Summary and results

The derivation and properties of the classical and the hyperbolic heat transfer equations have been studied. The starting points have been, on one side, the conservation of energy [1], and, on the other side, Fourier's law [1] for the CHE and Cattaneo's law [5] for the HHE. Approximate and exact solution methods have been given for both models. It has been observed that if vanishing Dirichlet conditions are considered, the HHE-solutions tend to their corresponding CHE-solution as the relaxation time decreases to zero. This has been observed by studying directly the solutions obtained with separation of variables and eigenfunction expansions. The same happens if flux or mixed boundary are considered.

In chapter 4 a theorem was given to approximate HHE-solutions with certain CHE-solutions, bounding the error by powers of the thermal relaxation time. This holds when periodic [16] or vanishing Dirichlet boundary conditions are considered. Therefore, when considering very small relaxation times, the Maxwell-Cattaneo model can be reduced to Fourier's model with a small error that is proportional to a power of τ_0. However, when considering the Dirichlet boundary conditions it turns out that the error obtained by the approximation is not proportional to any power of τ_0 except in trivial situations, and the result can only be applied to approximate the temperature.

In chapter 5 the laser radiation on a thin film has been studied. Four theoretical models were studied, starting from the classical heat equation with Dirichlet boundary conditions and ending with the HHE with an internal heat source and insulated boundaries. This final model displays interesting behaviours depending on the length of the heat pulse and the thickness of the film, in accordance with studies done by other authors [19, 20].

Chapter 6 reviews a study done by several scientists [28, 29, 30, 31] that discusses the HHE as the governing equation for a theoretical model of radiofrequency heating techniques on the cornea [33]. The result is that HHE should be considered in cases where the heat pulses are short in time. However, the results could vary if one considers a different model with more complicated geometries.

7.2 Limitations and thermodynamical analysis

The Maxwell-Cattaneo model is not frame-invariant, i.e., if the medium is moving, then the solutions also depend on the frame being used. This is avoided by Christov [11] by introducing the Christov-Cattaneo equations (3.25) and (3.28), and which are equivalent to the M-C equations if the medium is stationary.

On the other hand, once the dynamics of the M-C model have been studied, when wondering about its thermodynamical properties it turns out that the model does not fit in the scheme of *Classical Irreversible Thermodynamics (CIT)* [35], since entropy here may decrease in time in some situations. This violates the second law of thermodynamics, that states that in a thermodynamical process this quantity can never increase. For instance, this means that, according to Cattaneo's model, heat could be propagated from cold points to hot points in some situations. In fact, this was one of the first motivations to extend CIT to the so called *Extended Irreversible Thermodynamics (EIT)*, where the M-C Model does not show any controversy. However, when working on very small scales as, for instance, at molecular levels, where the particles' movement is assumed to be random, it is indeed possible that due to this Brownian motion this paradox predicted by the M-C model really happens.

The HHE has also been derived from a relativistic point of view, and actually in this scheme it is known as the *relativistic heat equation (RHE)* [34]. It turns out that in this relativistic form, the RHE is in accordance with CIT. Nevertheless, HHE and RHE are in the end the same equation. The difference relies on the derivation. While the first one is derived from a statistical mechanics point of view, the second one is deduced introducing a space like time $\tau = iCt$ and adapting Fourier's law and the conservation of mass to their relativistic form with the change

$$\nabla \to \Box = \partial_\tau \mathbf{o} + \partial_x \mathbf{i} + \partial_y \mathbf{j} + \partial_z \mathbf{k}. \tag{7.1}$$

7.3 Further work

The aim of this dissertation has been to give an overview of the Maxwell-Cattaneo model for non-Fourier heat conduction, and thus it is the first step for facing more complicated models in further research. The M-C model is one of the simplest known models that generalise Fourier's theory of heat transfer. Besides this one, the *Guyer-Krumhansl equations* [3] are also one of the most well known non-Fourier heat transfer models. In this case, 3 parameters are considered instead of 1 like in Cattaneo's model, although the HHE and hence the CHE can be obtained from the G-K equations by neglecting some terms when certain parameters tend to zero.

Both models can be derived from the celebrated *Boltzmann equation* [3, 35], which is a generally non-linear, integro-differential equation with the momentum of the particles as a new variable to be considered. Since this equation is too difficult to solve analitically, many easier models such as the M-C model or the G-K equations have been deduced by considering several simplifications.

In further studies we will examine these forms of heat equation and their validity at the nanoscale. For instance, the effect of other factors besides the relaxation time, such as nonlocalities or size dependent material properties have to be studied. Taking under consideration these parameters yields higher-order equations and hence adds more complexity to the model. On the other hand, we will worry about the length scale at which the classical heat equation is sufficiently accurate. Another issue will be considering the effect of boundary and initial conditions, we will have to study which are the appropiate conditions that should be set at the nano-scale.

Finally, the results of the mathematical study will be linked to experimental observations, to see if our theoretical results are confirmed by the experimental ones. Moreover, we will have to analyze any new behaviour predicted by the work and determine whether this be used to guide future nano-scale experiments or the design of nano-devices.

References

[1] S. Salsa, *Partial Differential Equations in Action. From Modelling to Theory*, Springer (2008).

[2] L. C. Evans, *Partial Differential Equations*, American Mathematical Society (1998)

[3] B. Straughan, *Heat Waves*, Springer (2011).

[4] L. Wang, X. Zhou, X. Wei, *Heat Conduction. Mathematical Models and Analytical Solutions*, Springer (2008).

[5] C. Cattaneo, *Sulla conduzione del calore*,Atti del Seminario Matematico e Fisico dell'Università di Modena 3 (1948), 3-21.

[6] P. Vernotte, *Les paradoxes de la théorie continue de l'équation de la chaleur*, Comptes Rendus de l'Académie des Sciences 246(22) (1958), 3154–3155.

[7] J. C. Maxwell, *On the Dynamical Theory of Gases*, Philosophical Transactions of the Royal Society of London 157 (1867), 49-88.

[8] T. G. Myers, *Optimizing the exponent in the heat balance and refined integral methods*, International Communications in Heat and Mass Transfer 36 (2009), 143-147.

[9] K. Termentzidis, S. Merabia, *Molecular Dynamics Simulations and Thermal Transport at the Nano-Scale*, Molecular Dynamics - Theoretical Developments and Applications in Nanotechnology and Energy (2012), 73-104.

[10] C. I. Christov, P. M. Jordan, *Heat Conduction Paradox Involving Second-Sound Propagation in Moving Media*, Physical Review Letters 94 (2005), 154301.

[11] C. I. Christov, *On frame indifferent formulation of the Maxwell-Catteneo model of finite-speed heat conduction*, Mechanic Research Communications 36 (2009), 481-486.

[12] M. Mustafa, *Cattaneo-Christov heat flux model for rotating flow and heat transfer of upper-convected Maxwell fluid*, AIP Advances 5 (2015), 047109.

[13] D. S. Chandrasekharaiah, *Hyperbolic thermoelasticity: a review of recent literature*, Applied Mechanics Reviews 51 (1998), 705-729.

[14] V. Peshkov, *Second sound in Helium II*, Journal Physics USSR (1944), 381-383.

[15] T.-M. Chen, *A hybrid transform technique for the hyperbolic heat conduction problems*, International Journal of Heat and Mass Transfer 63 (2013), 274-279.

[16] G. B. Nagy, O. E. Ortiz, O. A. Reula, *The behaviour of hyperbolic heat equation' solutions near their parabolic limits*, Journal of Mathematical Physics 35 (8) (1994).

[17] J. G. Fujimoto, J. M. Liu, E. P. Ippen, *Femtosecond laser interaction with metallic tungsten and non-equilibrium electron and lattice temperatures*, Physical Review Letters 53 (1984), 1837-1840.

[18] B. Stritzker, A. Pospieszyk, J. A. Tagle, *Measurement of lattice temperature of silicon during pulsed laser annealing*, Physical Review Letters 47 (1981), 356-358.

[19] S. Torii, W.-J.Yang, *Heat transfer mechanisms with laser heat source*, International Journal Heat Mass Transfer 48 (2005), 537-544.

[20] M. Lewandowska, L. Malinowski, *An analytical solution of the hyperbolic heat conduction equation for the case of a finite medium symetrically heated on both sides*, International Communications in Heat and Mass Transfer 33 (2006), 61-69.

[21] B. Vick, M. N. Ozisik, *Growth and decay of a thermal pulse predicted by the hyperbolic heat conduction equation*, Journal of Heat Transfer 105 (1983), 902-907.

[22] S. Roy, A.S. Vasedeva, R. B. Kudenatti, *Anumerical method for the hyperbolic-heat conduction equation based on multiple scale technique*, Applied Numerical Mathematics 59 (2009), 1419-1430.

[23] A. Erdélyi, W. Magnus, F. Oberhettinger, F.G. Tricomi, *Tables of Integral Transforms I*, Carolina Institute of Technology (1954).

[24] H. H. Pennes, *Analysis of tissue and arterial blood temperatures in the resting human forearm*, Journal Applied Physiology 85 (1998), 5-34.

[25] Z. S. Deng, J. Liu, *Numerical Simulation of 3-D Freezing and Heating Problems for Combined Cryosurgery and Hyperthermia Therapy*,Numerical Heat Transfer Applications 46 (6) (2004), 587-611 .

[26] K. Vafai, K. Khanafer, *Synthesis of mathematical models representing bioheat transport*, Advances in Numerical Heat Transfer 3 (2009), 1-28.

[27] M. M. Tung, M. Trujillo, J. A. Molina, M. J. Rivera, E. J. Berjano, *Modeling the Heating of Biological Tissue based on the Hyperbolic Heat Transfer Equation*, Mathematical and Computer Modeling 50 (2009), 665-672.

[28] M. Trujillo, J. A. Molina, M. J. Rivera, E. J. Berjano, *Effect of the thermal wave in radiofrequency ablation modeling: an analytical study*, Phys. Med. Biology 53 (2008).

[29] J. A. Molina, M. J. Rivera, M. Trujillo, F. Burdío, J. L. Lequerica, F. Hornero, E. J. Berjano, *Assessment of Hyperbolic Heat Transfer Equation in Theoretical Modeling for Radiofrequency Heating Techniques*, The Open Biomedical Engineering Journal 2 (2008), 22-27.

[30] E. J. Berjano, J. L. Alio, J. Saiz, *Modeling for radio-frequency conductive keratoplasty: implications for the maximum temperature reached in the cornea*, Physiological Measurements 26 (2005), 157-172.

[31] E. J. Berjano, E. Navarro, V. Ribera, J. Gorris, J. L. Alió, *Radiofrequency heating of the cornea: An engineering review of electrodes and applicators*, The Open Biomedical Engineering Journal 1 (2007), 71-76.

[32] A. Erez, A. Shitzer, *1980 Controlled destruction and temperature distributions in biological tissues subjected to monoactive electrocoagulation*, Journal of Biomechanical Engineering 102 (1980), 42–49.

[33] W. W. Haw, E. E. Manche, *Conductive keratoplasty and laser thermal keratoplasty*, International ophthalmology clinics 42(4) (2002), 99-106.

[34] Y. M. Ali, L. C. Zhang, *Relativistic heat conduction*, International Journal of Heat and Mass Transfer 48 (2005), 2397-2406.

[35] D. Jou, J. Casas-Vazquez, G. Lebon, *Extended Irreversible Thermodynamics*, Springer (2010).